NAZARBAYEV UNIVERSITY

PROLONGED INHIBITION OF CELL PROLIFERATION BY SHORT-TERM EXPOSURE TO CERTAIN ANTI-MITOTIC DRUGS

ARSEN ORAZBEK

(B.Sc. in Biological Sciences, Nazarbayev University)

A THESIS SUBMITTED IN PARTIAL FULFILLMENT OF THE REQUIREMENT OF NAZARBAYEV UNIVERSITY FOR THE DEGREE OF MASTER OF SCIENCE IN LIFE SCIENCES

APRIL 2025

Student:	**Arsen Orazbek** 	**25/04/2025**
Supervisor:	**Dr. Ivan Vorobyev**	**25/04/2025**

Examiners

The M.Sc. thesis of Arsen Orazbek has been approved by the examiners.

Professor Eugene Tulchinsky (NU, School of Medicine, eugene.tulchinsky@nu.edu.kz),

Professor Timo Burster (NU, School of Sciences and Humanities, Department of Biology, timo.burster@nu.edu.kz)

Declaration

I declare that the research contained in this thesis, unless otherwise formally indicated within the text, is my original work. The thesis has been written by me its entirety. I duly acknowledged all sources of information which have been used in the thesis. The thesis has not been previously submitted to this or any other university for a degree and does not incorporate any material already submitted for a degree.

Arsen Orazbek

25 April 2025

Acknowledgments

I would like to sincerely thank Dr. Ivan Vorobyev for his guidance, support, and valuable feedback throughout this project. I'm also grateful to my current and former lab colleagues — Marina Janibekova, Mariyam Kutchanova, Arlan Yelzhanov, Raushan Yeskendirova, Aruzhan Turlybek, and Mereke Suleimenov — for their help, teamwork, and everyday support in the lab. Thank you for the late-night data discussions, shared frustrations, and occasional jokes that helped me get through the toughest parts of the work.

I also want to thank Mikhail Chesnokov, Dana Muratovna, Yaroslav Abramenko, and Vadim Mustyatsa for their help during my learning period and for always being open to sharing their experience when I needed it.

Finally, I want to thank my family and friends for always being there for me, for their support, patience, and belief in me throughout this whole journey. I'm looking forward to the next steps ahead and am grateful to carry the experiences and lessons from this project with me.

Nazarbayev University, School of Science and Humanities, Department of Biology

Master's Degree Program in Biology
Arsen Orazbek: Prolonged Inhibition of Cell Proliferation by Short-Term Exposure to Certain Anti-Mitotic Drugs

BIOL 692 thesis; 46 pages, 4 appendices
Supervisor: Ivan Vorobyev, Professor of Biology, Nazarbayev University.
25.04.2025

Keywords: Mitotic inhibitors, proliferation arrest, cell cycle, mitotic arrest

Abstract

Mitotic inhibitors are widely used in cancer therapy to arrest rapidly dividing cells by disrupting spindle dynamics, yet most studies evaluate their effects under prolonged or continuous exposure, which does not reflect physiological conditions. *In vivo*, mitotic inhibitors are rapidly cleared through metabolism and excretion, making actual tumor exposure transient. The long-term cellular consequences of such short-term exposures, particularly in resistant cancer cells, remain poorly understood. This study investigates how brief (2-hour) treatment with various mitotic inhibitors—nocodazole, paclitaxel, epothilone B, vinorelbine, and SB-743921—affects the fate and proliferative capacity of A549 lung carcinoma cells. At T2 concentrations, all drugs effectively induced mitotic arrest, but their downstream outcomes differed. Epothilone B and vinorelbine promoted abnormal divisions and multinucleation, while SB-743921 primarily caused slippage, leading to large mononucleated cells. Despite drug washout and restoration of microtubule dynamics, normal mitosis remained suppressed for up to 6 days in most treatments except nocodazole. Life history analysis revealed delayed mitotic progression and abnormal outcomes after drug removal. Long-term monitoring showed delayed and drug-specific recovery: paclitaxel, vinorelbine, and SB-743921 led to gradual proliferation recovery, while epothilone B caused persistent arrest. Ki67 staining and β-galactosidase assays confirmed that short-term treatments induced prolonged proliferative arrest and senescence. These findings challenge the assumption that sustained drug exposure is required for efficacy and emphasize the lasting impact of even brief mitotic inhibition. By revealing how short exposures affect recovery, this study supports the design of clinically relevant, personalized regimens that optimize tumor cell targeting while reducing toxicity and improving patient outcomes.

Abbreviations

Noc	Nocodazole
Vin	Vinorelbine
PTX	Paclitaxel
EpoB	Epothilone B
SB	SB-743921
MTA	Microtubule-targeting agents
PBS	Phosphate-Buffered Saline
FBS	Fetal Bovine Serum
TMRM	Tetramethylrhodamine Methyl Ester
PLK1	Polo-like kinase 1
DMSO	Dimethyl sulfoxide
GFP	Green Fluorescent Protein

Table of Contents

Introduction

Mitosis

Eukaryotic cell division proceeds through a tightly regulated sequence of events known as the cell cycle. This cycle comprises four major phases: G1 phase, S phase, G2 phase, and M phase. The G1, S, and G2 phases are referred to as interphase, during which the cell grows and replicates its DNA. Specifically, the G1 and G2 phases serve as gap phases for cellular growth and biosynthetic activities, while the S phase is dedicated to the replication of chromosomal DNA (Alberts et al., 2022).

The M phase represents the shortest segment of the cell cycle, typically lasting about one hour in a 24-hour cell cycle of human culture cells. Despite its brevity, the M phase is crucial, as it encompasses mitosis (the division of the nucleus) and cytokinesis (the division of the cell itself).

Mitosis is further divided into five distinct stages: prophase, prometaphase, metaphase, anaphase, and telophase. During prophase, chromosomes condense, and each consists of two tightly associated sister chromatids. Simultaneously, the mitotic spindle, a dynamic structure composed of microtubules and associated motor and non-motor proteins, begins to assemble in the cytoplasm. In prometaphase, the nuclear envelope breaks down, allowing spindle microtubules to attach to chromosomes via specialized protein complexes called kinetochores (Alberts et al., 2022).

As cells progress into metaphase, chromosomes align at the metaphase plate, a central plane equidistant from the spindle poles. The mitotic spindle at this stage consists of three main classes of microtubules: kinetochore microtubules, which connect centrosomes to the kinetochores on chromosomes; non-kinetochore (interpolar) microtubules, which interact with microtubules from the opposite pole to help elongate the cell; and astral microtubules, which extend from the centrosomes to the cell cortex and assist in spindle positioning (Figure 1). The spindle apparatus ensures that sister chromatids are correctly bi-oriented before the spindle assembly checkpoint allows transition into anaphase, where chromatids are pulled apart. Finally, in telophase, nuclear envelopes reform around the separated chromosome sets, and the cell prepares for cytokinesis (Alberts et al., 2022).

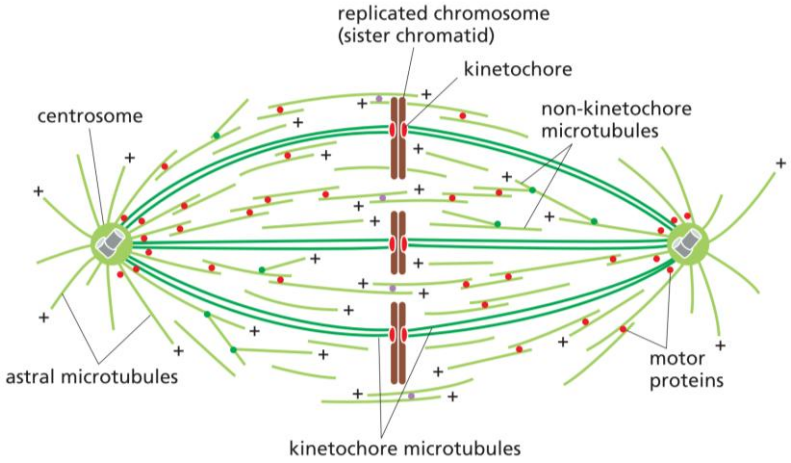

Figure 1. The illustration of the mitotic spindle during metaphase (Alberts et al., 2022)

Mitotic Inhibitors

Mitotic inhibitors are a diverse class of compounds that block mitosis by preventing the transition from metaphase to anaphase, often leading to cell death. Because of their higher proliferation rates, cancer cells are more sensitive to these drugs than normal cells, making mitotic inhibitors effective chemotherapeutic agents. These inhibitors target proteins essential for spindle formation and chromosome segregation, including tubulins, mitotic kinesins, PLK1, and Aurora A and B kinases (Škubník et al., 2020; Fig. 1). This research focuses on two primary classes of mitotic inhibitors: microtubule-targeting agents and Eg5 kinesin inhibitors.

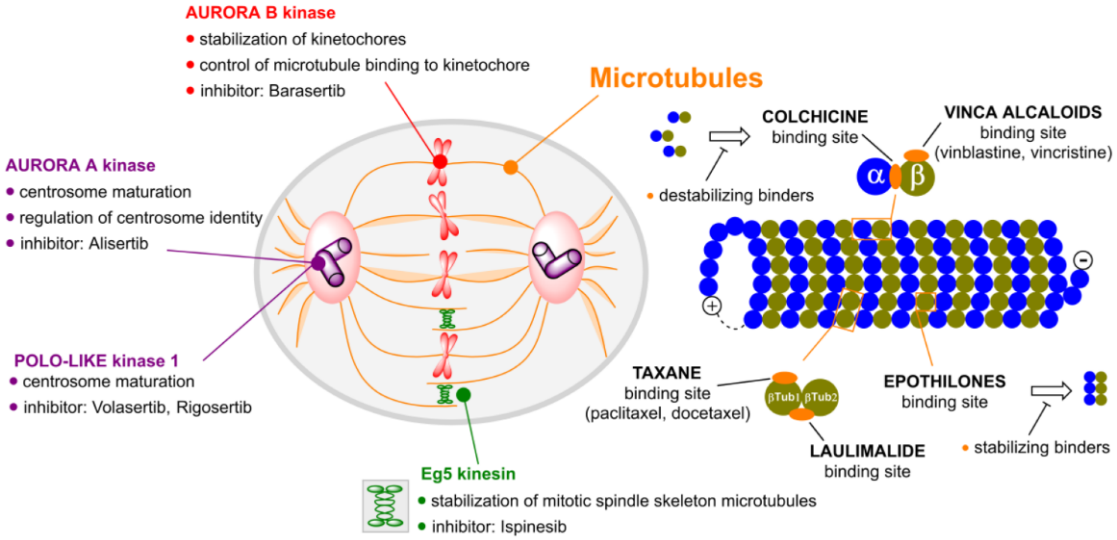

Figure 2. Illustration of molecular targets of different mitotic inhibitors (Škubník et al., 2020)

Microtubule Targeting Agents

Among mitotic inhibitors, antimicrotubule agents are especially notable for their clinical use in cancer therapy. These agents are categorized into two main types: microtubule-destabilizing agents, which bind to tubulin subunits to inhibit microtubule polymerization, and microtubule-stabilizing agents, which prevent microtubule depolymerization (Fanale et al., 2015). Both types disrupt the dynamic assembly and disassembly of microtubules, a process essential for proper chromosome segregation and cellular organization during mitosis. This disruption impairs cell division and often leads to cell death (Čermák et al., 2020).

Microtubule-destabilizing agents include nocodazole (Noc) and vinorelbine (Vin). Nocodazole has limited clinical application due to relatively low clinical efficacy, but it is widely used for research purposes (Laisne et al., 2021). On the other hand, vinorelbine is FDA-approved and used to treat non-small cell lung, breast, and ovarian cancers (Gregory & Smith, 2000).

Conversely, microtubule-stabilizing agents like paclitaxel (PTX) and epothilone B (EpoB) bind to β-tubulin within microtubules, promoting their assembly and stabilization and preventing depolymerization (Kowalski et al., 1997). PTX is a widely used chemotherapeutic drug to treat multiple cancers like ovarian, breast, cervical, pancreatic, and lung cancers (Sati et al., 2024). Epothilone B, though not yet clinically approved, shows promise due to its enhanced efficacy in

eliminating solid tumors compared to PTX (Čermák et al., 2020). Its analog, ixabepilone, received FDA approval in 2007 for treating metastatic and chemoresistant breast cancer, underscoring the therapeutic potential of this drug class (Egerton, 2008).

Mitotic Kinesin Inhibitor

SB-743921 (SB) is a targeted mitotic kinesin inhibitor that specifically binds to Eg5 (also known as Kinesin-5 or KIF11), a kinesin motor protein critical for forming the bipolar mitotic spindle (Bongero et al., 2015). Eg5 ensures proper chromosome alignment and separation during mitosis, and SB-743921 inhibition of the ATP binding site of Eg5 disrupts spindle formation and function, leading to mitotic arrest (Lad et al., 2008). Unlike antimicrotubule agents, mitotic kinesin inhibitors are associated with fewer adverse side effects, such as neurotoxicity and alopecia, which makes it an attractive candidate for cancer therapy (Gomez et al., 2011). However, the general efficacy of most Eg5 inhibitors against solid tumors has been limited, largely due to challenges in achieving sufficient therapeutic concentrations for tumor suppression (Komlodi-Pasztor et al., 2012). Despite this, SB-743921 remains a promising agent, particularly for aggressive, rapidly dividing tumors such as glioblastoma, where therapeutic effects may be enhanced by combining it with targeted delivery strategies (Gampa et al., 2020).

Cellular Responses to Mitotic Inhibitors

Antimitotic agents at therapeutic concentrations are known to induce mitotic arrest, effectively halting cell proliferation by activating the spindle assembly checkpoint. Following this arrest, cells either undergo mitotic cell death or experience mitotic slippage, a process in which cells exit mitosis without proper chromosome segregation and cytokinesis (Figure 2; Weaver, 2014). Mitotic slippage results in the formation of polyploid cells with either a single enlarged nucleus or multiple nuclei (Was et al., 2022). In some cases, cells may complete cytokinesis without proper chromosome segregation, producing progeny with abnormal nuclear content—either multinucleated or polyploid—which is referred to as abnormal division. These abnormal cells may undergo delayed cell death, enter a senescent state, or persist for extended periods. A subset of slippage-derived cells can arrest in the G1 phase of the subsequent cell cycle, particularly if key regulatory checkpoints (e.g., p53 pathway) are functional, preventing further proliferation and contributing to long-term cell cycle arrest or senescence (Bharadwaj & Mandal, 2019).

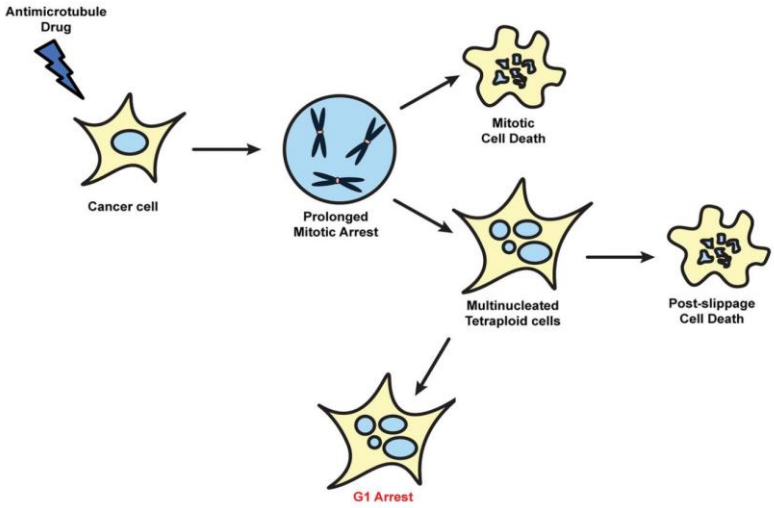

Figure 3. Mitotic outcomes after treatment with antimicrotubule agents. Adapted from Weaver, 2014

Our previous study (Suleimenov et al., 2022) demonstrated that cellular responses to microtubule-targeting agents are threshold-dependent. Two critical thresholds were defined: T1, the maximum ineffective dose at which more than 90% of cells divide normally, and T2, the minimal effective dose at which more than 90% undergo mitotic arrest. Based on responses to T2 concentrations, cell lines were categorized into two groups: (a) sensitive cells (e.g., HeLa and HaCaT), in which most cells undergo death following mitotic arrest, and (b) resistant cells (e.g., A549 and PC-3), where most cells evade death via mitotic slippage.

Importantly, the study by Suleimenov et al. (2022) confirms that at concentrations above the T2 threshold, resistant cell lines such as A549 consistently exhibit high frequencies of mitotic slippage across a wide dose range, with relative proportions of mitotic outcomes remaining stable even with a 30-fold increase in drug concentration. This suggests that above the mitostatic threshold, drug dose has little effect on shifting cell fate in resistant populations. The study also emphasized that inter- and intra-line differences dominate the variability in mitotic response, with each cell line showing a conserved fate profile that is drug independent. These findings highlight that the mitotic outcome is determined more by cell-intrinsic properties than by the type or dose of antimitotic drug used.

Aims of the Thesis Project

Research Gap

Although most of the previous studies had focused mainly on long-period treatments with antimitotic agents, these studies often fail to account for real-world scenarios. In living organisms, drug clearance occurs naturally, with small amounts of the administered drug being eliminated from the body daily. Although it is known that Nocodazole washout results in the restoration of cell behavior as normal cell division continues (Novais-Cruz et al., 2023), the cellular response to a treatment followed by washout with other mitotic inhibitors is still unknown.

Hypothesis

Short-term exposure of A549 cells to various antimitotic agents, including microtubule-targeting drugs (excluding Nocodazole) and mitotic kinesin inhibitors, will induce a prolonged arrest in cell proliferation, with the extent and duration of this arrest differing based on the specific agent applied.

Aims

1. **To determine effective mitotic arrest-inducing concentrations (T2) of various antimitotic agents and characterize their immediate cellular effects**
   While T2 doses—those inducing mitotic arrest in >90% of cells—are known for some drugs, a systematic comparison of mitotic outcomes across multiple inhibitors in resistant A549 cells is lacking (Suleimenov et al., 2022). This study identified T2 concentrations for five drugs, including Epothilone B and SB-743921, and compared mitotic fates (death, normal mitosis, abnormal mitosis, which includes mitotic slippage and abnormal division) under continuous exposure.
2. **To evaluate the reversibility of drug effects after short-term exposure and washout**
   Although Nocodazole treatment followed by washout is known to result in recovery of normal mitotic divisions (Novais-Cruz et al., 2023), less is known about how other inhibitors behave after brief treatments. Here, we analyzed mitotic outcomes after 2-hour and 16-hour treatments followed by washout.
3. **To investigate the long-term consequences of short-term drug exposure on cell fate and proliferation**
   Previous studies have examined the long-term consequences of continuous treatment with mitotic inhibitors, demonstrating that cells can recover and resume proliferation (Mittal et al., 2017; Mirzayans et al., 2018). However, the long-term dynamics of short-term drug treatment followed by washout remain poorly understood, particularly in resistant cancer cells. We assessed clonogenicity, distribution of mononucleated and multinucleated cells, proliferation capacity, and senescence over 18 days after washout.

Materials and Methods

Cell Culture and Treatments

A549 human lung carcinoma cells (ATCC) were maintained in Dulbecco's Modified Eagle Medium (DMEM, Gibco, 11965092) supplemented with 10% fetal bovine serum (Fetal Bovine Serum Advanced, Heat Inactivated (HI), Collected in South America, FBS-HI-11A) and 1% penicillin-streptomycin (Gibco, 15140122) at 37°C in a humidified 5% CO_2 atmosphere. Cells were treated with mitotic inhibitors at the following concentrations: 1 μM nocodazole (Noc, Sigma-Aldrich, 31430-18-9), 300 nM paclitaxel (PTX, Sigma-Aldrich, T7191-5mg), 10–30 nM epothilone B (EpoB, Sigma-Aldrich, 152044-54-7), 1 μM vinorelbine (Vin, Sigma-Aldrich, V2264-5mg), and 10 nM SB-743921 (SelleckChem, S2182). These concentrations are T2 (minimal dose where 90% of cells are arrested in mitosis) or higher concentrations The negative control group was treated with 0.05% dimethyl sulfoxide (DMSO, Thermo Scientific Chemicals, J66650.AK).

Titration of EpothiloneB and SB-743921

200,000 cells were seeded into 6-well plates and cultured for 2 days before being treated with increasing drug concentrations (0.1, 0.3, 1, 3, 10, and 30 nM) for 48 hours without washout. Following treatment, cells were trypsinized and fixed in 70% cold ethanol for at least 2 hours. Fixed cells were then treated with RNase A (Thermo Scientific, EN0531) and stained with 1.5 μM propidium iodide (Invitrogen, P1304MP). DNA content was analyzed using an Attune NxT flow cytometer, and the data were processed with FlowJo v10.10 software.

Live-Cell Imaging of Abnormal Outcomes

1000 cells were seeded into μ-Slide 8 Well Glass Bottom treated with inhibitors. Then, they were stained with 50 nM tetramethylrhodamine methyl ester (TMRM, Invitrogen, 15656139) and 5 μM Hoechst 33342 (Invitrogen, 15932344). The μ-Slide 8 Well Glass Bottom was observed under live microscopy (100×, NA 1.47) for 48 hours post-washout using time-lapse microscopy at 30-minute intervals. Obtained images were processed via ImageJ software and Adobe Photoshop.

Live-Cell Imaging of Cells Under the Treatment of Mitotic Inhibitors

10,000 cells were seeded into 12-well plates and stained with 50 nM TMRM and 5 μM Hoechst 33342 prior to treatment with mitotic inhibitors. Time-lapse imaging was performed using an Axioscope Observer 5 microscope equipped with a 20×, NA 0.5, Neofluar objective. Images were acquired every 30 minutes for 48 hours (Ex: 546 nm/Em: 567 nm). Mitotic events were analyzed using ImageJ software, with 100 cells per treatment group classified into categories: normal mitosis, mitotic slippage, abnormal division, or cell death.

Live-Cell Imaging of Cells After Treatment of Mitotic Inhibitors Followed by Washout

Cells treated with inhibitors for 2 or 16 hours were stained with 50 nM TMRM and 5 μM Hoechst 33342 and tracked for 48 hours post-washout using time-lapse microscopy at 30-minute intervals. Mitotic outcomes were categorized as normal mitosis, mitotic slippage, abnormal division, or cell death, with 100 cells analyzed per group using ImageJ.

Drug Washout and Microtubule Dynamics Analysis

1000 cells were seeded into μ-Slide 8 Well Glass Bottom treated with inhibitors for 2 or 16 hours, followed by two PBS washes and one DMEM (10% FBS, 1X l-glutamine 1X, and 1% penicillin-streptomycin) wash. Microtubule dynamics post-washout were assessed by transfecting A549 cells with an EB3-GFP plasmid (AddGene, #190164) using GeneJect 39 (Molecta). Transfected cells were treated with inhibitors for 2 hours, washed, and imaged at 0, 2, and 24 hours post-washout using time-lapse spinning disc fluorescence microscopy (100×, NA 1.47, 2-second intervals). Microtubule growth was quantified by analyzing 10 comets from each of nine cells per treatment group (three cells from each biological repeat), generating kymograms in ImageJ using the KymoReslice plugin. The protocol for measuring EB3-GFP comet speed was adapted from Mustyatsa et al. (2019). Statistical analysis was performed using one-way Brown-Forsythe ANOVA with Dunnett's T3 post hoc test.

Assessment of the Ratio of Multinucleated and Mononucleated Cells

Cells were seeded into 12-well plates at a density of 10,000 cells per well and allowed to adhere for 2 days. Following this, cells were treated with mitotic inhibitors for 2 hours, after which a washout procedure was performed. Cells were then monitored on days 0, 1, 3, 6, 9, 12, 15, and 18 post-washout to assess long-term morphological changes, including multinucleation, polyploidy, and nuclear abnormalities. For imaging, cells were stained every 3 days with 5 μM Hoechst 33342 and 50 nM TMRM and visualized using wide-field microscopy (Axio Observer 5, 10× objective, NA 0.5, Neofluar, Ex: 546 nm / Em: 567 nm). At least 100 cells per treatment group were manually analyzed using ImageJ software.

Proliferation Assessment

Cells were seeded into 12-well plates at a density of 10,000 cells per well. After 24 hours, drugs were added for 2 hours and subsequently washed out. To assess long-term proliferation, cells were fixed with 4% paraformaldehyde on days 0, 1, 3, 6, 9, 12, 15, and 18 after washout. Proliferative capacity was evaluated using Ki67 immunostaining. Fixed cells were permeabilized with 0.1% Triton X-100, incubated with an anti-Ki67 primary antibody (Abcam, ab15580), and detected using an HRP-conjugated anti-rabbit secondary antibody (Abcam, ab6721). Hematoxylin was used as a nuclear counterstain. Then, they were imaged under a bright field microscope (10X, NA 0.5). The proportion of Ki67-positive cells was quantified to determine the extent of proliferation over time.

Senescence Assessment

10,000 cells were seeded into 12-well plates. After 24 hours, drugs were added for a 2-hour treatment, followed by washout. Seven days after washout, cells were fixed with 4% paraformaldehyde and stained using a senescence-associated β-galactosidase (SA-β-gal) staining assay (Cell Signaling Technology, #9860) at pH 6.0. Stained cells were imaged under bright-field microscopy (10X, NA 0.5), and at least 100 cells/treatment group were counted to determine the proportion of SA-β-gal-positive cells.

Statistical Analysis

All experiments were conducted with at least three biological replicates unless otherwise specified. Quantitative data are presented as mean ± standard deviation (SD) for normally distributed datasets, and as median ± SD for non-normally distributed data. Data normality was evaluated using the Shapiro–Wilk test, and appropriate parametric or non-parametric statistical tests were applied accordingly. Homogeneity of variances was assessed using Levene's test in Microsoft Excel 365. For comparisons involving multiple groups, one-way ANOVA followed by Tukey's post hoc test was used for parametric data, depending on the comparison type. For non-parametric data, the Kruskal–Wallis test followed by Dunn's post hoc test was applied. Statistical analyses were performed using GraphPad Prism 8. Statistical significance was defined as $p < 0.05$ ($p < 0.05$ = *, $p < 0.01$ = **, $p < 0.001$ = ***, $p < 0.0001$ = ****).

Results

Defining Effective Doses of Mitotic Inhibitors

Previous research on dose-dependent responses to microtubule-targeting agents across various cell lines identified two critical concentration thresholds, T1 and T2, which define cellular responses. The T2 dose corresponds to the minimum concentration required to induce mitotic arrest in more than 90% of cells (Suleimenov et al., 2022). Cell lines such as A549, PHF, 3T3, and PC3 have been characterized as relatively resistant to microtubule inhibitors, with a higher survival rate at T2 and above, compared to more sensitive lines like HeLa. For this study, we selected the A549 cell line and employed drug concentrations equal to or exceeding the T2 threshold to ensure robust mitotic arrest while minimizing cytotoxicity. Based on our prior work, we selected 1 μM Nocodazole, 1 μM Vinorelbine, and 300 nM Paclitaxel as standard mitotic inhibitors, all of which meet or exceed the T2 dose in A549 cells.

In addition to these drugs, we also wanted to evaluate Epothilone B, a microtubule stabilizer, and SB-743921, a kinesin Eg5 inhibitor. Dose-response analysis revealed that T2 concentration (>90% mitotic arrest) for Epothilone B starts from 30 nM, while for SB-743921 it starts from 10 nM. The flow cytometry analysis also proves that these are T2 concentrations that we used for our next research steps (Figure 4, Supplementary Figure 1).

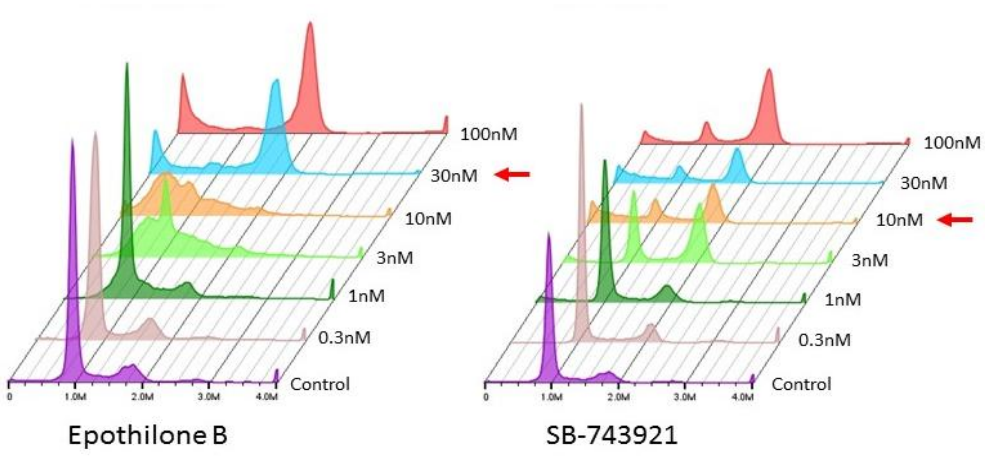

Figure 4. Titration of Epothilone B and SB-743921 in A549 cells. DNA content histograms after 24-hour treatment with increasing concentrations of Epothilone B (left) and SB-743921 (right). Arrows indicate selected T2 concentrations (30 nM for Epothilone B, 10 nM for SB-743921) that induce mitotic arrest (significant accumulation in G2/M) (N> 30,000).

Mitotic Outcomes Following Treatment with Antimitotic Agents

Treatment with these agents resulted in three primary mitotic outcomes: mitotic slippage, abnormal division, and death in mitosis (Figure 5). Mitotic slippage was the most frequent, leading to the formation of either multinucleated or enlarged mononucleated cells. These outcomes occur when cells exit mitosis without proper chromosome segregation or cytokinesis. In some cases, we also observed abnormal divisions, in which cells complete cytokinesis but produced at least two daughter cells with aberrant nuclear content, such as polyploidy or multinucleation.

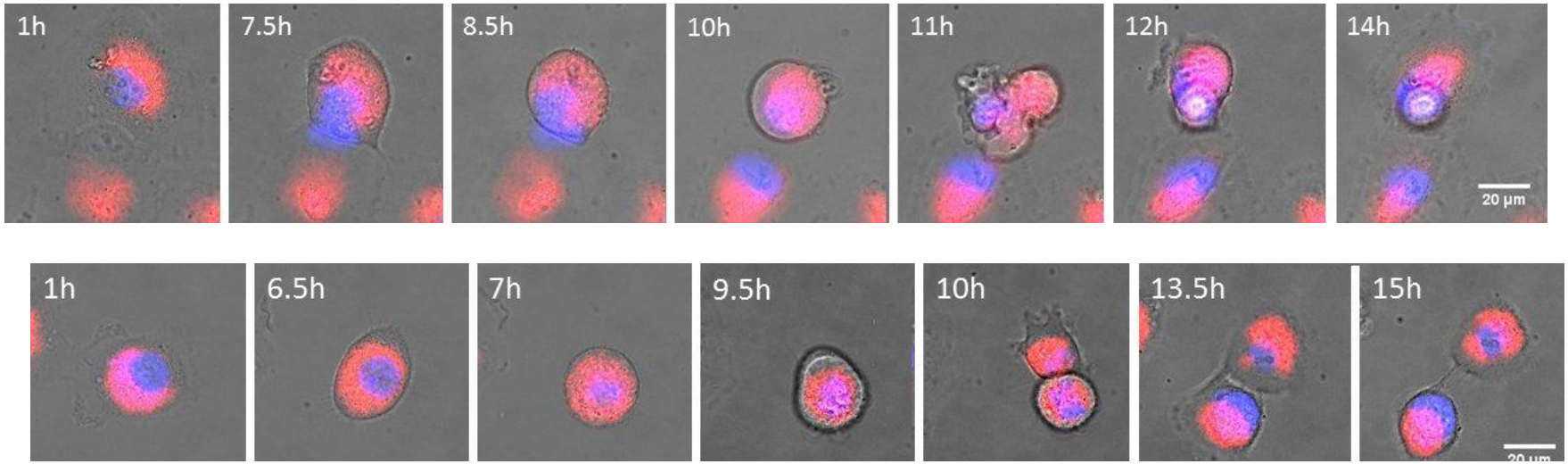

Figure 5. Mitotic slippage (A) and abnormal division (B) of A549 cells after treatment with 30nM EpoB. DNA content was visualized via 5uM Hoechst stain (blue), and mitochondrial membrane potential was visualized by staining with 50 nM TMRM (green). Scale bar = 20 µm. Time is given in hours.

Further titration revealed compound-specific differences in the dose-dependence of mitotic arrest and outcome (Figure 6). At low concentrations (0.1–0.3 nM), Epothilone B allowed 80–90% of cells to divide normally. SB-743921 permitted a similar fraction of normal mitosis only at 0.1 nM, with a sharp drop to less than 10% at 0.3 nM. At 1 nM, Epothilone B induced mitotic arrest in ~70% of cells, which often resulted in abnormal divisions, while SB-743921 at the same dose caused mitotic arrest in ~70–80% of cells, and death in mitosis is about 20%. At higher concentrations (3–30 nM), both compounds nearly eliminated normal mitosis. However, SB-743921 consistently caused a greater proportion of mitotic arrest associated with cell death, whereas Epothilone B primarily led to arrest followed by slippage.

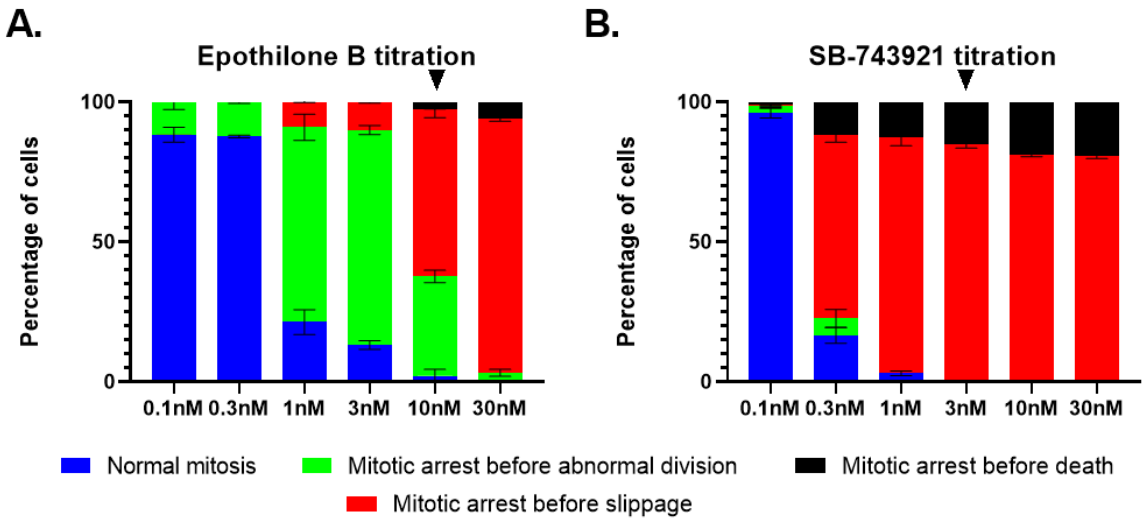

Figure 6. Distribution of events after treatment of cells with different concentrations of A) EpoB and B) SB-743921 drugs. N>100. The black arrow depicts the T2 dose.

At the selected concentrations for all drugs, we did not observe any normal divisions (Figure 7). In control (untreated) conditions, nearly all cells divided normally; however, treatment with Nocodazole, Paclitaxel, Vinorelbine, and SB-743921 resulted in mitotic slippage as the dominant outcome, occurring in approximately 80–90% of cells. A smaller fraction of cells (5–15%) died in mitosis across all treatments. Notably, Epothilone B was the only compound to permit a measurable proportion of cells (about 5%) to undergo abnormal division. It was also observed that mitotic slippage during SB-743921 treatment predominantly led to the formation of large mononucleated cells (more than 70% large mononucleated cells), while other treatments more commonly resulted in multinucleated cells following slippage or abnormal division (less than 5% large mononucleated cells).

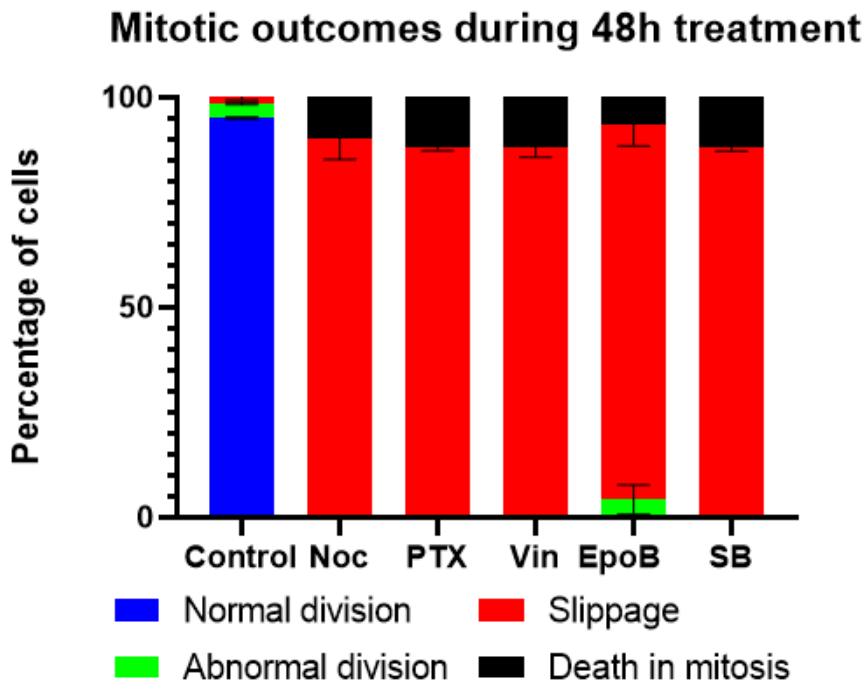

Figure 7. Mitotic outcomes during 48-hour treatment with T2 concentrations of different anti-mitotic drugs (N=100). Bars represent the percentage of cells undergoing normal division (blue), slippage (red), abnormal division (green), or death in mitosis (black).

In addition to bar charts (Figure 7), cell behavior is also depicted using life history plots, which include not only cells that exited mitosis but also those that remained arrested or never entered mitosis (Figure 8). Each plot tracks individual rounded cells from the start of mitotic rounding. Under Paclitaxel, Epothilone B, and Vinorelbine, many cells remain in mitosis for extended periods before slippage (red) or death (black), while some divide abnormally (green). If the cell fate ends as a result of cell death, the horizontal bar ends. If cells did not enter mitosis, their fate is represented as purple horizontal bars throughout the whole observation.

Life history plots reveal that most cells treated with anti-mitotic drugs remained rounded in mitosis for extended periods before slippage or death, with mitotic duration often exceeding 20 hours (Figure 8). In contrast, control cells typically completed mitosis rapidly, within an hour after rounding. Under Nocodazole, Paclitaxel, Vinorelbine, and SB-743921, slippage was the most common outcome, with cells maintaining a rounded morphology for a prolonged time before returning to interphase without division. Death in mitosis occurred throughout the timeline but usually after extended mitotic arrest. Importantly, life history plots also show that a minority of cells—approximately 5–10%—remained in a mononucleated interphase state for the entire observation period and never entered mitosis.

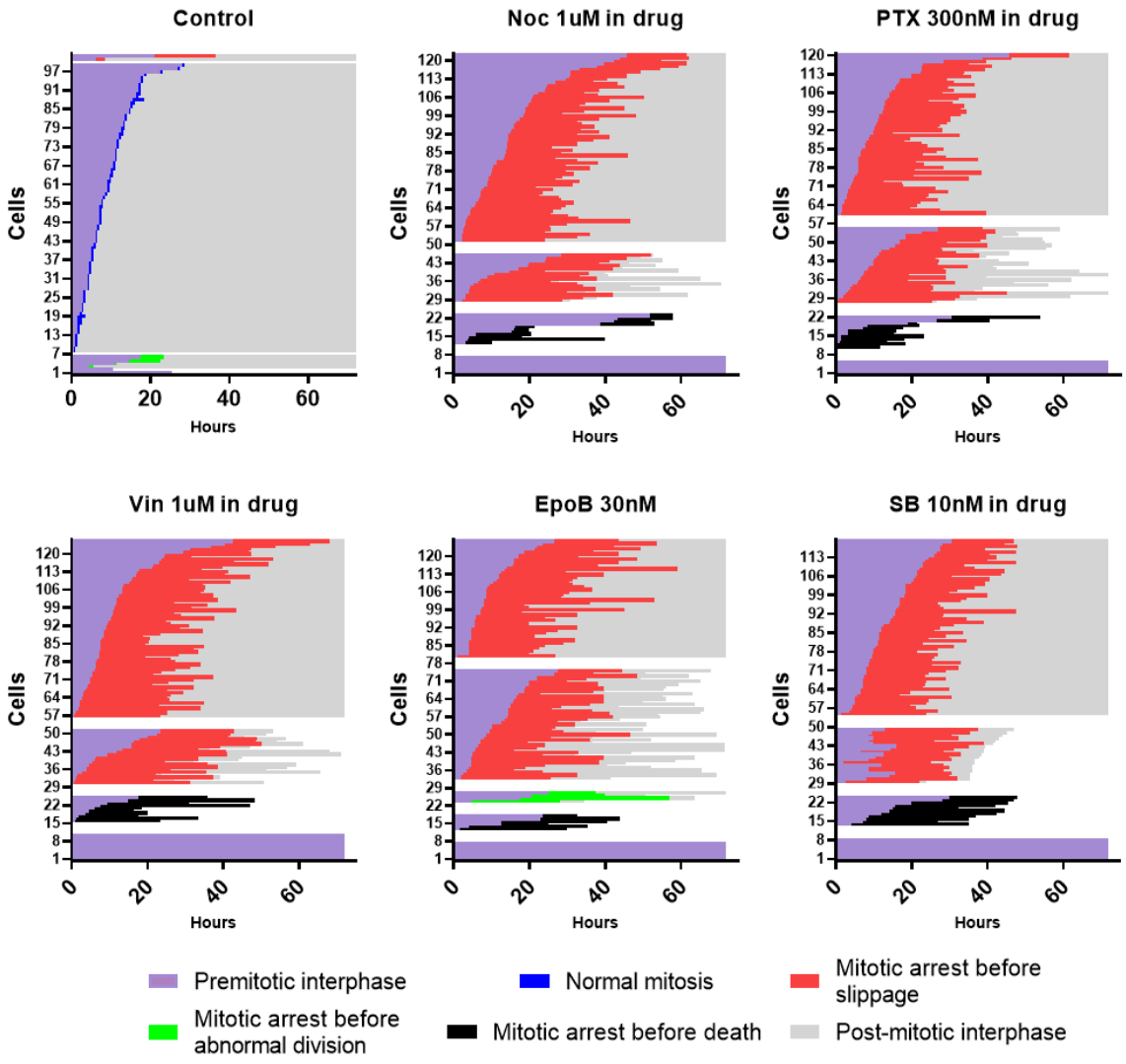

Figure 8. Individual life histories of mononucleated A549 cells during 72h treatment. N>100. The x-axis represents the duration after the drug washout. Color-coded by phase: pre-mitotic interphase (purple), normal mitosis (blue), mitotic arrest before slippage (red), mitotic arrest before abnormal division (green), mitotic arrest before death (black), and post-mitotic interphase (grey). Only the first mitotic outcome was recorded for each cell. Cells were treated with the indicated drugs or left untreated (control) and imaged continuously for 48 hours (N>100).

Persistence of Abnormal Mitosis After Drug Washout

While it is well-established that Nocodazole washout leads to the restoration of normal cell behavior and resumption of typical mitosis, the effects of washout from other mitotic inhibitors are less understood. Therefore, we wanted to check how drug washout affects cell behavior after 16-hour treatment followed by washout.

As we removed drugs, in all treatment groups we observed two distinct cell populations: rounded mitotic cells that had already entered mitosis before washout and mononucleated interphase cells that can enter mitosis after washout. >70% of cells in the population are still rounded after drug treatment followed by washout, and others are mononucleated cells (Figure 9). The percentage of multinucleated cells was low for all treatment groups (<1%, not shown).

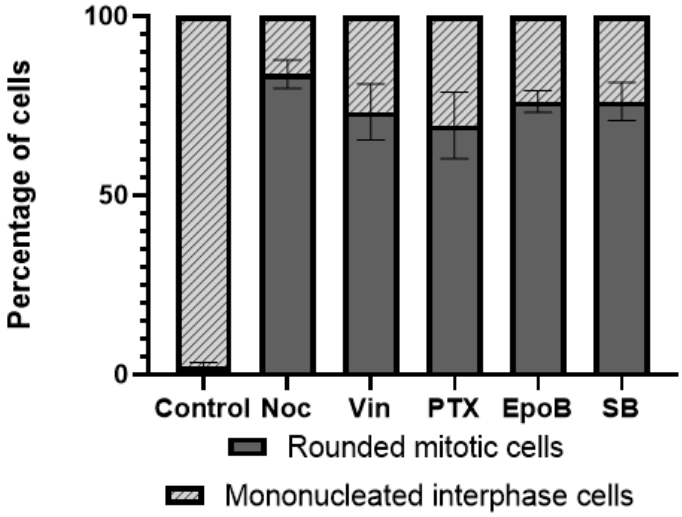

Figure 9. Proportion of mitotic and interphase cells after 16-hour drug treatment followed by washout (N=100).

Given the common belief that mitotic inhibitors primarily affect cells that enter mitosis, we sought to explore the extent to which this holds true by comparing the behavior of mitotically arrested cells (cells that had already entered mitosis before washout) with mononucleated interphase cells (cells that entered mitosis after washout).

After 16 hours of treatment followed by washout, the behavior of rounded mitotic cells differs depending on the drug (Figure 10). Rounded cells after Nocodazole treatment followed by washout can undergo normal mitosis (39.2±0.5%). In contrast, treatments after Paclitaxel, Epothilone B, Vinorelbine, and SB-743921 followed by washout only resulted in abnormal mitosis. After Paclitaxel, Epothilone B, and Vinorelbine treatments followed by washout, there was 20-35% abnormal division, 35-60% mitotic slippage, and 10-20% death in mitosis. On the other hand, SB-743921 treatment followed by washout lacked abnormal division (71.9±0.9% slippage and 28.1±0.9% death in mitosis).

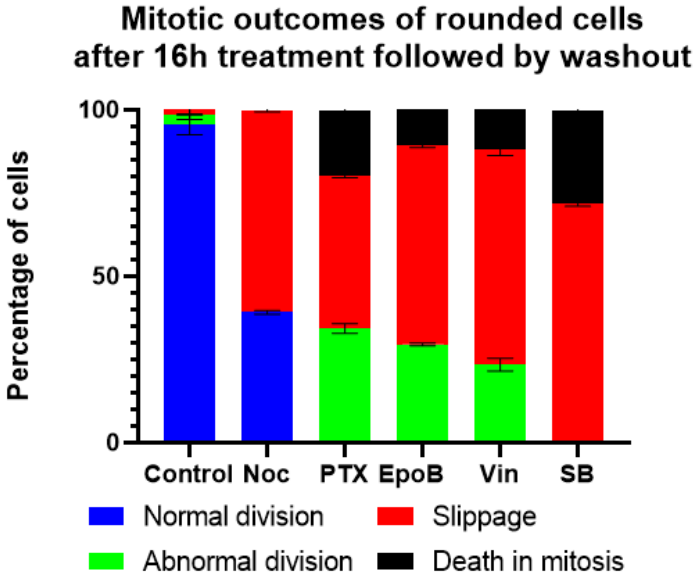

Figure 10. Distribution of mitotic outcomes among rounded mitotic A549 cells (i.e., cells that entered mitosis before drug removal) after 16-hour treatment followed by washout (N=100).

Life history chart (Figure 11) shows that A549 cells already in mitosis at the time of drug washout remained rounded for extended periods across all treatments, indicating sustained mitotic arrest. While the duration of arrest varied between drugs, SB-743921 and Vinorelbine caused the longest mitotic delays, often exceeding 20 hours. Nocodazole-treated cells exited mitosis more quickly, while Paclitaxel and Epothilone B led to intermediate arrest durations. The timing of mitotic resolution was highly variable among cells, highlighting heterogeneous recovery dynamics even after short-term drug exposure.

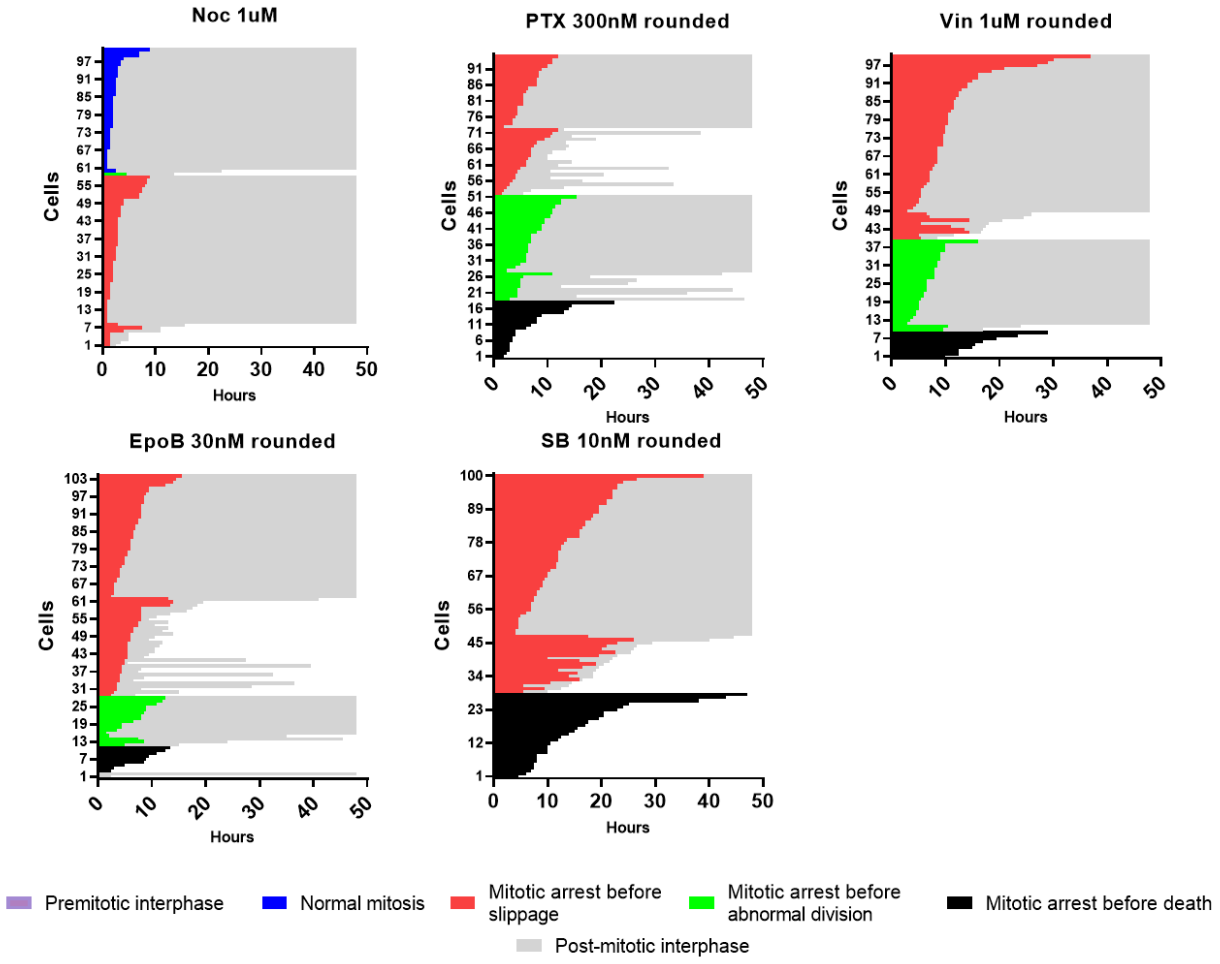

Figure 11. Individual life histories of rounded mitotic A549 cells after 16h drug treatment followed by washout. Observation time is 48h. N=100. The x-axis represents the duration after the drug washout.

Despite the removal of drugs, the mononucleated interphase cells did not undergo normal division (except Nocodazole) (Figure 12). The results from the life history analysis reveal distinct differences in how A549 cells respond to various mitotic inhibitors after a 16-hour treatment followed by washout. Drug-specific differences in prior mitotic outcomes are evident among mononucleated interphase cells observed after 16 hours of treatment. Nearly all mononucleated cells result from normal mitosis in the control and Nocodazole-treatment groups. In contrast, Paclitaxel and Epothilone B treatments followed by washout lead to a mix of outcomes where 66.6±1.0% and 42.9±1.0% are abnormal divisions and 25.6±0.3% and 49.5±1.4% are mitotic slippages, respectively. Vinorelbine and SB-743921 treatment followed by washout results show almost absent or absent abnormal divisions; instead, nearly all mononucleated cells reflect slippage (54.5±2.3% % for Vin, 76.6±1.4% for SB) or result from cells that eventually die in mitosis (43.0±2.0% and 23.4±1.4%, respectively).

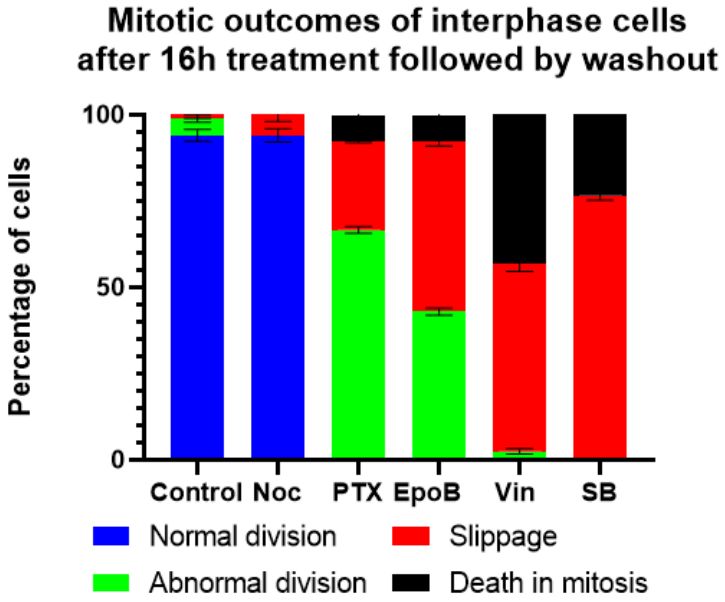

Figure 12. Distribution of mitotic outcomes among mononucleated interphase A549 cells (i.e., cells that had entered mitosis after drug removal) after 16-hour treatment followed by washout (N=100).

Life history plots in Figure 13 depict the behavior of mononucleated A549 cells that entered mitosis after drug washout, following a 16-hour treatment with antimitotic agents. Across all drug conditions, there was a delay in mitotic entry, with many cells remaining in interphase (purple) for extended durations before attempting division. The timing of mitotic entry varied substantially among cells and treatments, reflecting heterogeneous recovery kinetics as was observed for rounded cells. Under Nocodazole, most cells progressed into mitosis relatively early and behaved similarly to control cells. In contrast, cells treated with Paclitaxel, Epothilone B, Vinorelbine, and SB-743921 followed by washout, entered mitosis more slowly. Additionally, the duration of mitotic arrest/mitosis is slightly higher for Nocodazole, Paclitaxel, and Epothilone B treatment groups compared to the duration of mitosis in the control. On the other hand, cells treated with Vinorelbine and SB-743921 followed by washout had much longer mitotic arrest durations.

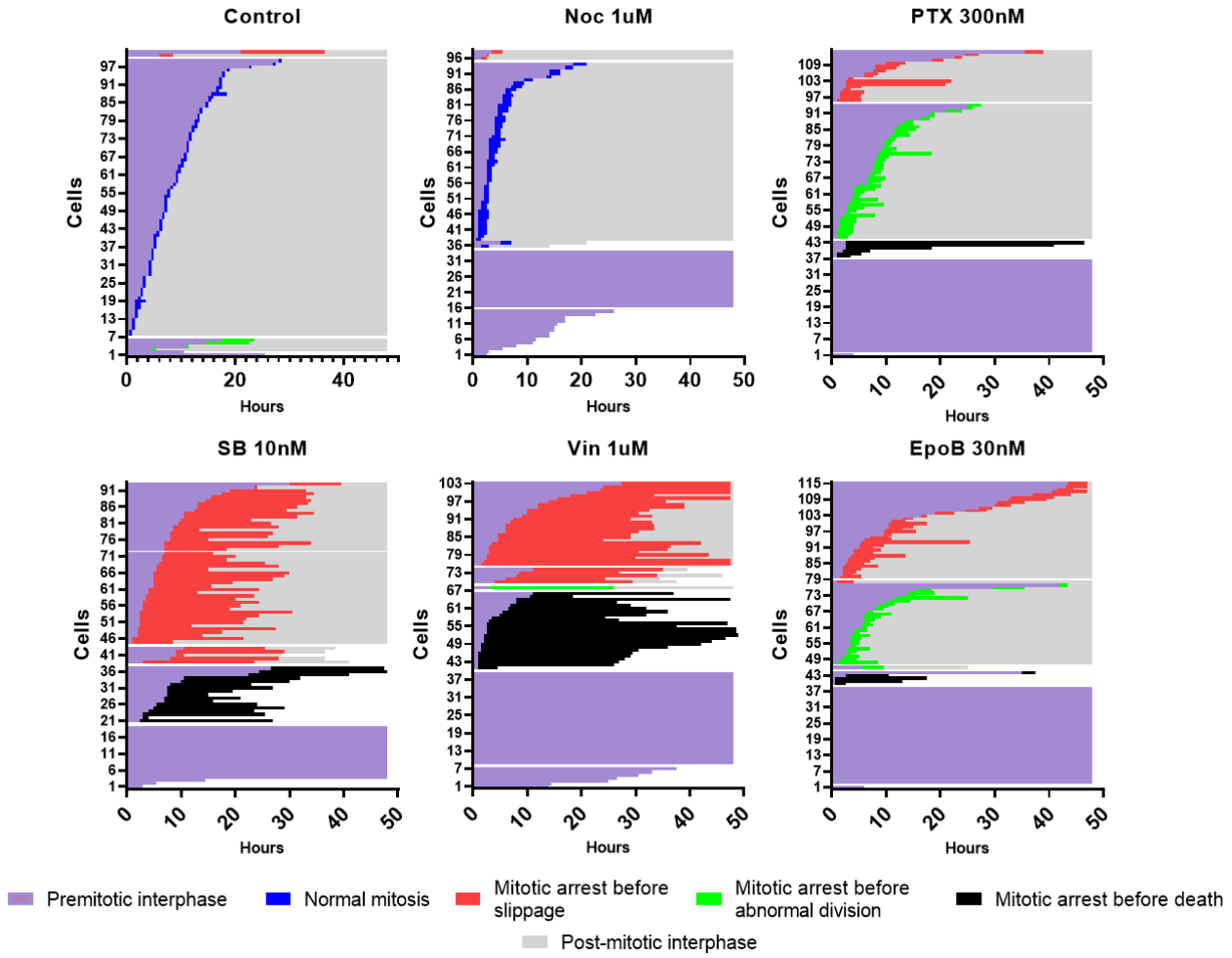

Figure 13. Individual life histories of mononucleated A549 cells after 16h drug treatment followed by washout. Observation time is 48h. N=100. The x-axis represents the duration after the drug washout.

Shorter Drug Exposure Is Sufficient to Induce Abnormal Mitosis

Since a 16-hour duration of drug treatment followed by washout was sufficient for abnormal mitosis, we wanted to check whether a shorter drug treatment duration in the form of a 2-hour treatment with subsequent washout is sufficient to have the same result. In both the control and Nocodazole groups, nearly all cells underwent normal division, with only a small proportion showing abnormal division, slippage, or death in mitosis.

In contrast, 2h treatment followed by washout from other agents resulted in the absence of normal mitosis. Paclitaxel-treated cells displayed a marked shift in mitotic outcomes compared to Nocodazole treatment: 17.5±1.5% of cells underwent slippage, and abnormal division occurred in 82.5±1.5% of the population. For Epothilone B, 53.5±1.3% of cells slipped from mitosis, with the remaining cells undergoing abnormal division (46.5±1.3%). In Vinorelbine and SB-743921 treatment groups, slippage dominated the mitotic outcomes (82.7±0.3% and 91.3±0.6%, respectively).

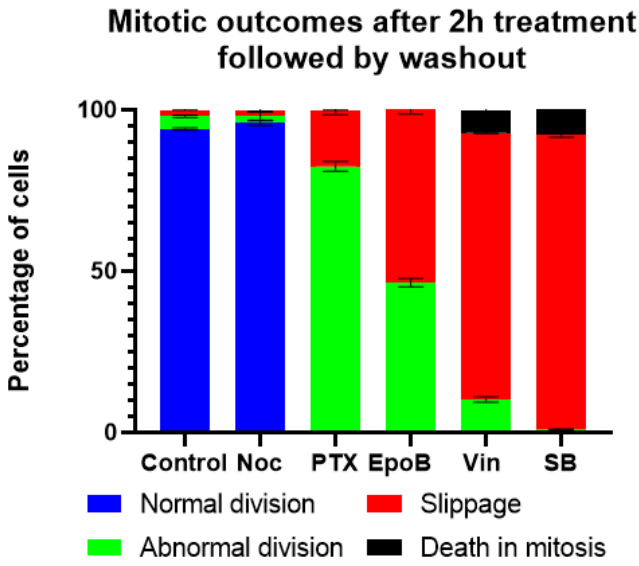

Figure 14. Distribution of mitotic outcomes among mononucleated interphase A549 cells (i.e., cells that had entered mitosis after drug removal) after 2-hour treatment followed by washout (N=100).

Life histories (Figure 15) revealed distinct differences in mitotic entry timing and arrest duration across treatments. In control and Nocodazole-treated cells, mitotic entry was rapid and synchronous, with short arrest durations. Paclitaxel and Epothilone B induced delayed mitotic entry and slightly prolonged mitotic arrest, where median mitotic arrest durations are 2.5 ± 3.1 h and 1.5±0.9h, respectively. In contrast, Vinorelbine and SB-743921 also caused delayed mitotic entry and prolonged mitotic arrest compared to other groups (12.5 ± 6.0 h and 14.5 ± 4.7 h, respectively).

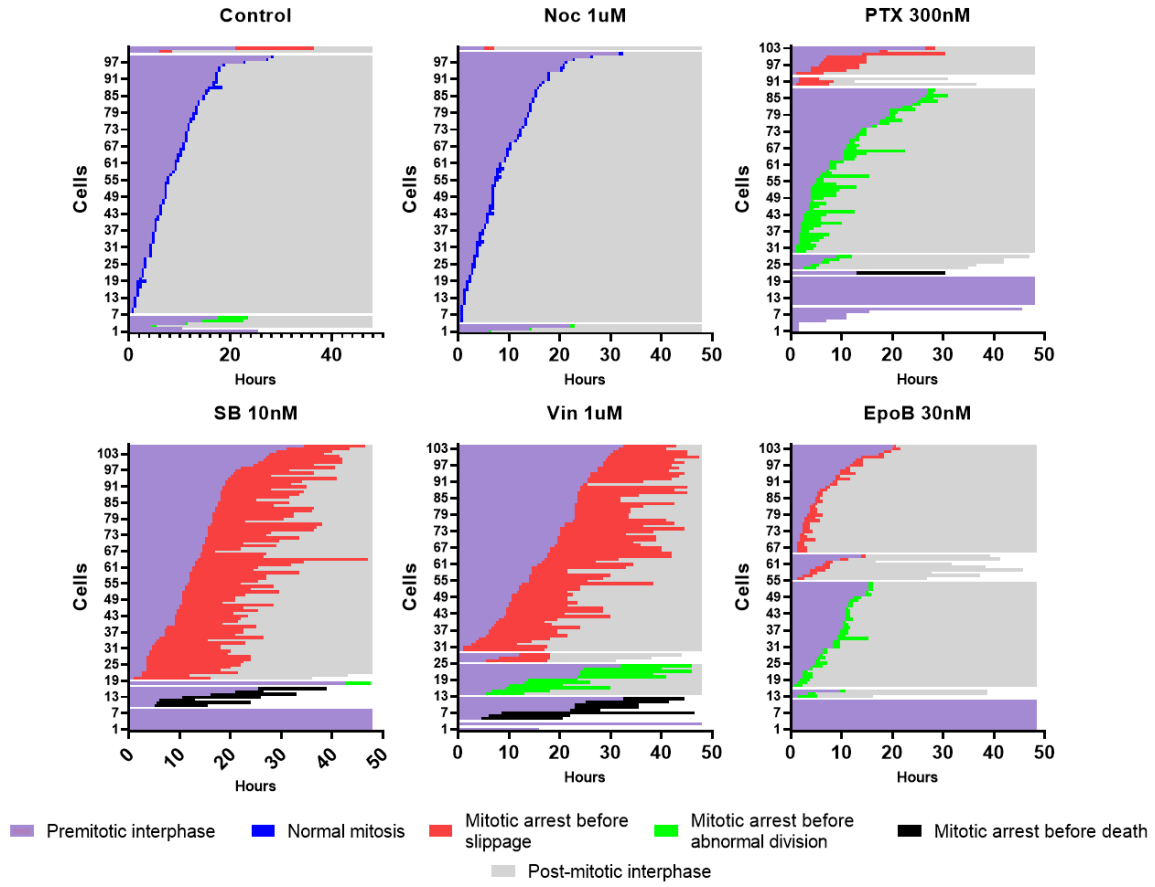

Figure 15. Individual life histories of mononucleated A549 cells after 2h drug treatment followed by washout. Observation time is 48h. N=100. The x-axis represents the duration after the drug washout.

Overall, there were no significant differences between these treatments since both treatments resulted in abnormal mitosis (Figures 14 and 15). The only difference of shorter duration was the incidence of cell death (>20%) and a lower proportion of mononucleated cells (>15%) that failed to enter mitosis within 48 hours after 2h treatment followed by washout, compared to the proportion after 16h treatment followed by washout. Normal cell behavior was absent for at least 6 days after washout, since there was no increase in cell number after 2h Paclitaxel, Epothilone B, Vinorelbine, and SB-743921 followed by washout (Figure 16, Supplementary Table 1), demonstrating the absence of normal mitosis.

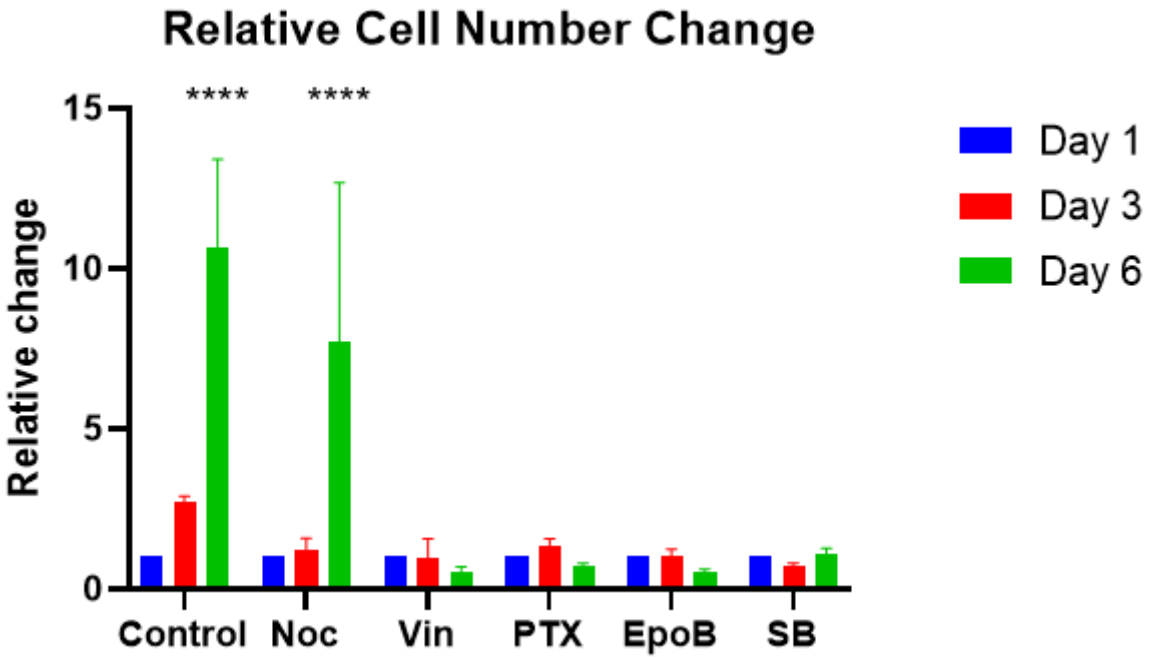

Figure 16. Relative cell number changes after 2-hour drug treatment followed by washout. Cell numbers were measured on Day 1 (blue), Day 3 (red), and Day 6 (green) post-washout and normalized to Day 1. Statistical analysis: one-way Kruskal–Wallis's test with Dunnett's multiple comparison test (**** is $p < 0.0001$).

As a 2-hour drug treatment following washout was sufficient to induce abnormal mitosis, we next aimed to explore the consequences of short-term exposure in more detail. Specifically, we examined: (1) how efficiently the drugs were removed and (2) how the duration of mitotic arrest compared between short-term treatment followed by washout (16h and 2h) and continuous treatments.

As we observed abnormal mitosis even after short-term drug treatment followed by washout, we sought to evaluate how effectively drug washout restored the primary function of microtubule-targeting agents—namely, the disruption of microtubule dynamics. To assess this, we employed the EB3 comet assay, a live-cell imaging approach that tracks the movement of EB3-GFP protein comets, which bind to the growing plus-ends of microtubules and serve as sensitive markers of microtubule polymerization activity. The speed and presence of EB3 comets directly reflect the dynamic state of microtubules. Immediately after washout, all microtubule-targeting agents (Paclitaxel, Epothilone B, Vinorelbine, and Nocodazole) resulted in the complete disappearance of EB3-GFP comets, confirming their effective suppression of microtubule dynamics. However, within 24 hours post-washout, EB3-GFP comets reappeared, and their growth speed returned to levels comparable to untreated controls, indicating that microtubule polymerization activity was fully restored (Figure 17, Supplementary Table 2).

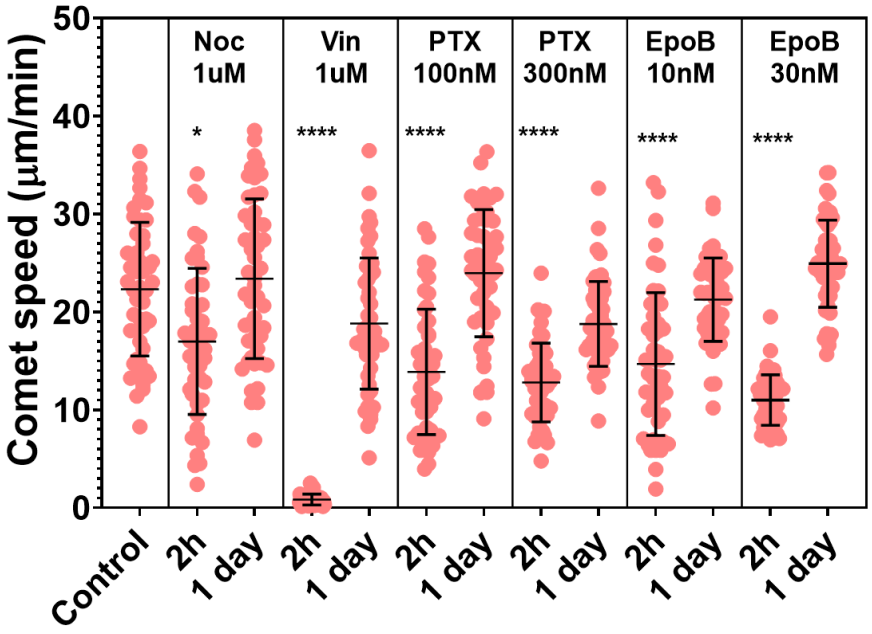

Figure 17. EB3 comet speed in mononucleated A549 cells after 2-hour drug treatment followed by washout. Comet speed was measured 2 hours and 1 day after washout from the indicated drugs: Nocodazole (1 µM), Vinorelbine (1 µM), Paclitaxel (100 nM and 300 nM), and Epothilone B (10 nM and 30 nM). A total of 90 comets were measured from 9 cells per group. All data were normally distributed. Statistical significance: one-way ANOVA with Tukey's multiple comparisons test. **** is $p < 0.0001$.

We assessed the duration of mitotic arrest in A549 cells exposed to different mitotic inhibitors under three treatment conditions: continuous 48-hour exposure ("in drug"), and short-term 2-hour or 16-hour treatments followed by drug washout (Table1, Figure 18, Supplementary Table 3). Control cells exhibited minimal mitotic arrest, with median durations below 2 hours.

Among all treatments, Nocodazole (1 µM) induced the most prolonged mitotic arrest during continuous exposure, with a median duration of 22 ± 8.4 hours. However, following 2-hour or 16-hour treatments followed by washout, the arrest duration dropped to 0.5 ± 0.3 hours and 1.5 ± 0.5 hours, respectively—comparable to the duration of normal mitosis in control cells (0.5 ± 1.4 hours)—indicating full recovery of mitotic progression.

Paclitaxel (300 nM) and Epothilone B (30 nM) also caused significant mitotic arrest during continuous treatment, with median durations of 16 ± 5.8 hours and 21 ± 7.9 hours, respectively. After 2-hour or 16-hour exposures followed by washout, mitotic arrest durations were reduced but remained longer than control (Paclitaxel: 2.5 ± 3.1 h and 2.5 ± 2.8 h; Epothilone B: 1.5 ± 0.9 h and 3 ± 3.8 h), suggesting partial restoration of mitotic exit.

In contrast, Vinorelbine (1 µM) and SB-743921 (10 nM) showed minimal reduction in mitotic arrest duration following drug removal. Even after 2-hour or 16-hour treatments followed by washout, the arrest durations remained substantially longer than those observed for other drug groups (Vinorelbine: 12.5 ± 6.0 h and 27 ± 6.7 h; SB-743921: 14.5 ± 4.7 h and 19 ± 6.0 h, respectively).

Table 1. Duration of mitotic arrest (in hours) in A549 cells across control and treatment conditions

Treatment	Duration	Median durations ± SD
Control		0.5±1.4h
Nocodazole	Continuous	22±8.4h
	16h followed by washout	1.5±0.5h
	2h followed by washout	0.5±0.3h
Paclitaxel	Continuous	16±5.8h
	16h followed by washout	2.5±2.8h
	2h followed by washout	2.5±3.1h
Epothilone B	Continuous	21±7.9h
	16h followed by washout	3±3.8h
	2h followed by washout	1.5±0.9h
Vinorelbine	Continuous	23±6.7h
	16h followed by washout	27±6.7h
	2h followed by washout	12.5±6.0h
SB-743921	Continuous	20±4.7h
	16h followed by washout	19±6.0h
	2h followed by washout	14.5±4.7h

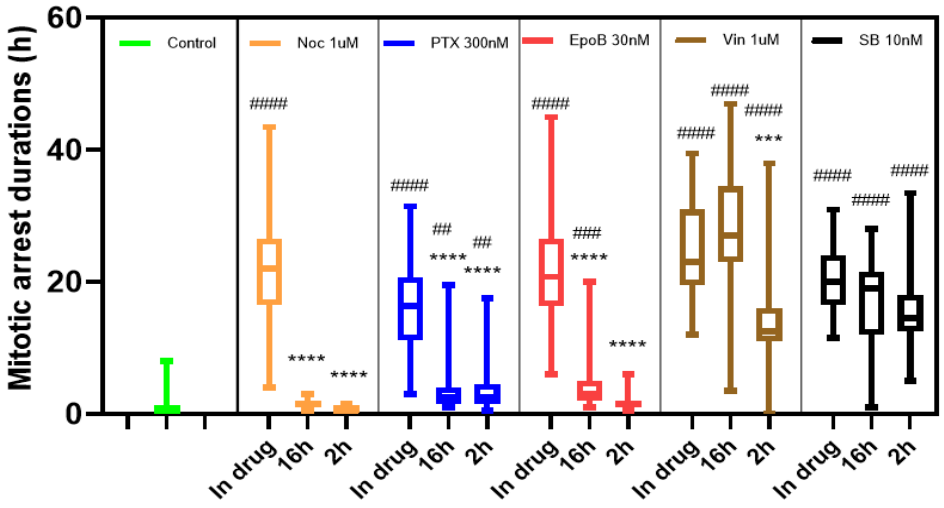

Figure 18. Duration of mitotic arrest (in hours) in A549 cells across control and treatment conditions. Box plots show the duration of mitotic arrest during continuous 48-hour drug exposure ("In drug"), and after 2-hour and 16-hour treatments followed by washout. Data are shown for each drug: Nocodazole (1 μM), Paclitaxel (300 nM), Epothilone B (30 nM), Vinorelbine (1 μM), and SB-743921 (10 nM). N = 50 cells per condition. # symbols indicate statistically significant differences between each treatment group and the control, while * symbols indicate comparisons between short-term (2 h or 16 h) and continuous ("in drug") treatments. Statistical significance was determined using a one-way Kruskal–Wallis's test followed by Dunnett's multiple comparison test. **** or #### indicate $p < 0.0001$.

The Long Cell Proliferation Arrest After Short-Term Drug Treatment Followed by Washout

While previous studies have shown that cells can regain proliferative capacity after continuous drug treatment (Mittal et al., 2017; Mirzayans et al., 2018), the effects of shorter treatment durations have not been systematically examined. Since a 2-hour treatment followed by washout was sufficient to induce abnormal mitosis, and normal mitosis was absent by Day 6 after washout in Paclitaxel, Epothilone B, Vinorelbine, and SB-743921 treatment groups, we sought to determine whether cells could eventually recover normal proliferative behavior.

To address this, we monitored cell populations for up to 18 days after washout for any signs of recovery in normal cell behavior (Table 2). We observed two distinct recovery patterns: recovery in the form of colonies and dispersed growth. Colony formation was defined as the emergence of densely packed clusters consisting of approximately 30 or more cells, indicating localized and sustained proliferation (Figure 19B). In contrast, dispersed growth was characterized by scattered, individual mononucleated cells or small patches (typically fewer than 10 cells) spread across the surface (Figure 19A, 19C, and 19D).

In cells treated for 2 hours, different patterns of recovery were observed. Nocodazole (1 μM) treatment followed by washout led to dispersed growth immediately after washout, indicating minimal disruption of recovery. Paclitaxel (300 nM) induced limited colony formation by Day 12. Vinorelbine (1 μM) produced small patches of 10–15 cells on Day 12, with colonies forming by Day 15. SB-743921 (10 nM) led to colony formation by Day 12. In contrast, Epothilone B (30 nM) showed the absence of any recovery even for 30 days (Figure 19E).

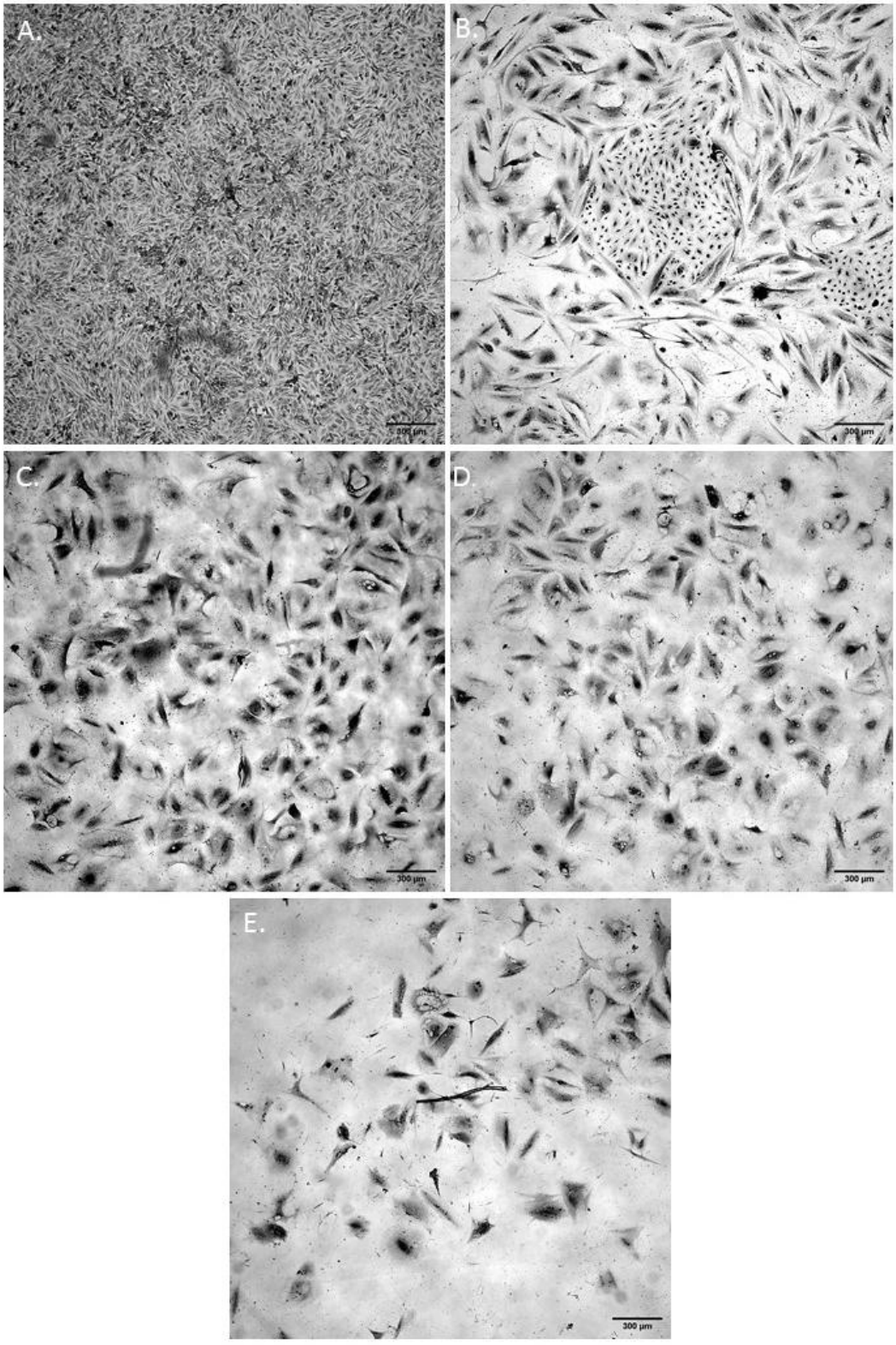

Figure 19. Brightfield images of A549 cells 15 days after 2-hour drug treatment followed by washout. Images demonstrate the representative fields for each treatment condition: (A) Nocodazole (1 µM), (B) Paclitaxel (300 nM), (C) Vinorelbine (1 µM), (D) SB-743921 (10 nM), and (E) Epothilone B (30 nM). (5×, NA=0.16, scale bars: 300 µm).

Table 2. Timing and pattern of A549 cell recovery after 2-hour drug treatment followed by washout.

Drug	Start of recovery	Form of recovery
Nocodazole	No change	Dispersed
Paclitaxel	Day 10±1.73	Colonies
Vinorelbine	Day 13±1.73	Dispersed
SB-743921	Day 14±1.73	Dispersed
Epothilone B	No recovery for 30 days	none

Since we know that mitotic slippage and abnormal divisions result in either multinucleated or large mononucleated cells, we wanted to assess the dynamics of these cells after drug washout (Figure 20).

In control and Nocodazole-treated cells, the percentage of mononucleated cells remained consistently high (95-99%) from Day 1 to Day 6, with minimal emergence of multinucleated or large mononucleated cells. In contrast, all other drug treatments led to a marked decline in the mononucleated population starting from Day 1 post-washout. Between Days 3 and 6, the percentage of mononucleated cells reached its lowest levels (10–25%) across all treatments, with multinucleated cells becoming the predominant population. A gradual recovery of the mononucleated population was observed from Day 9 onward in the Paclitaxel, SB-743921, and Vinorelbine groups, reaching near-complete restoration (about 90% mononucleated population) by Days 15 to 18. In contrast, cells treated with Epothilone B failed to recover, with the mononucleated population remaining below 10% even 18 days after washout.

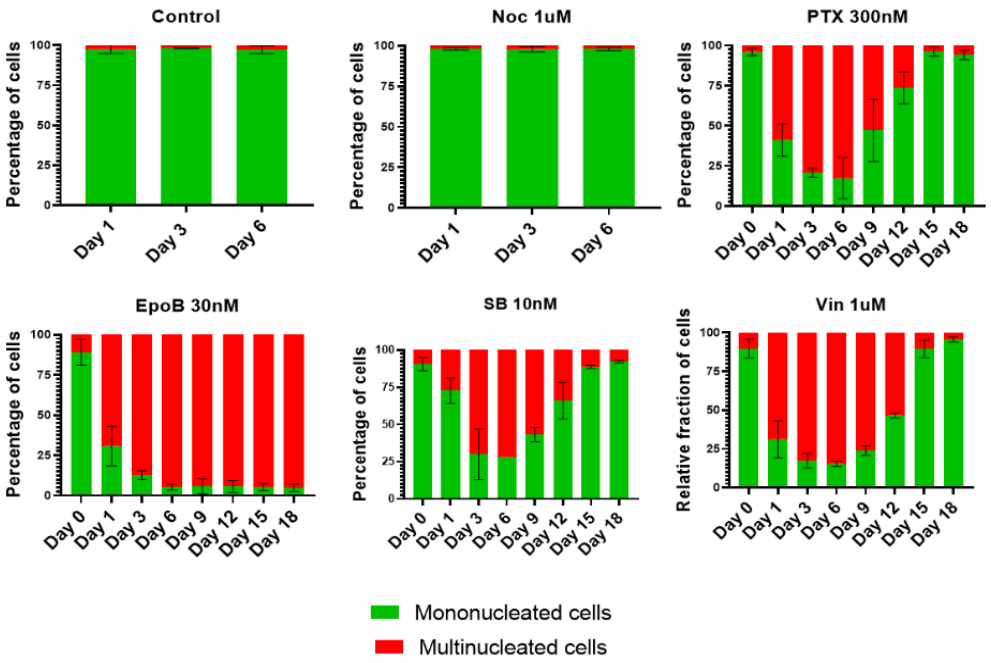

Figure 20. The dynamics of the multinucleated/large mononucleated and mononucleated A549 cell ratio after washout from 2h incubation in different drugs (n>300).

To further evaluate whether the observed decrease in the mononucleated cell population was associated with impaired proliferative capacity, we assessed Ki67 expression — a marker of cell proliferation — over time following drug washout (Figure 21). After Nocodazole treatment followed by washout, the majority of cells remain Ki67-positive across all time points, as in the control group. In contrast, after Paclitaxel, Epothilone B, SB-743921, and Vinorelbine treatment followed by washout, there was an increase in Ki67-negative cells starting from Day 3, reflecting a reduction in proliferation. Among these, Epothilone B shows the strongest and most persistent effect, with only less than 5% of cells remaining Ki67-positive up to Day 18. Paclitaxel, SB-743921, and Vinorelbine show a reduction in proliferation (10-20% Ki67 positive cells) only until Day 6 after washout, and starting from Day 9 after washout, slow recovery of proliferative cells was observed. By Days 15 and 18, full recovery proliferation was observed. These results suggest that short-term exposure to certain mitotic inhibitors can lead to prolonged suppression of proliferation in a drug-dependent manner.

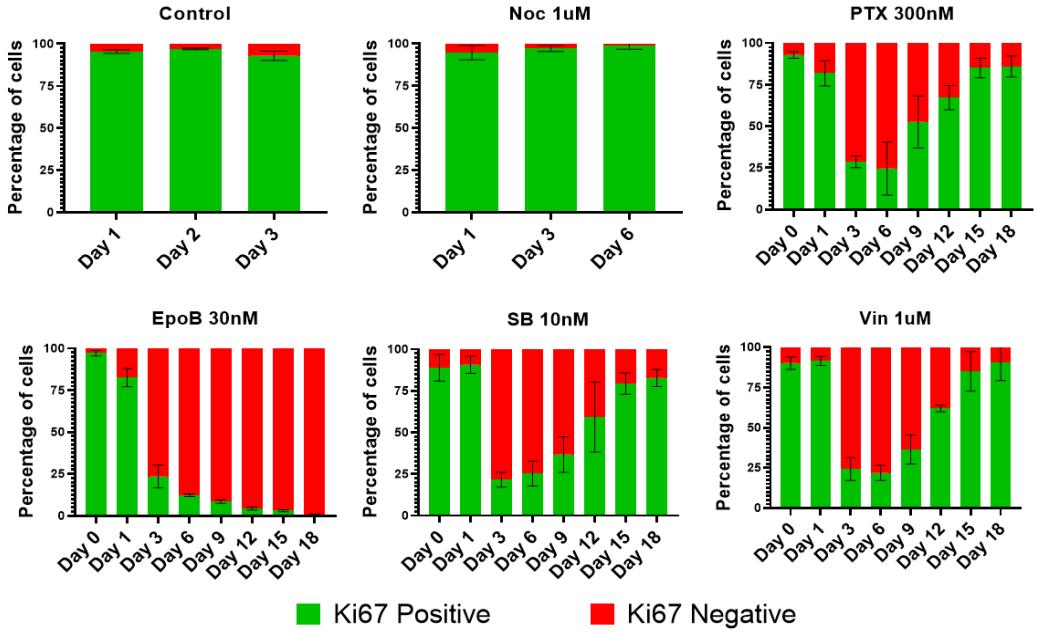

Figure 21. The ratio of actively proliferating cells after 2-hour drug treatments followed by washout (N > 300). Ki67-positive cells represent those that were able to proliferate, while Ki67-negative cells indicate those that were not able to proliferate**.**

To complement our long-term proliferation analysis, β-galactosidase staining was performed on Day 7 after washout to assess treatment-induced senescence (Figures 22 and 23). This point was selected based on the observation that Ki67 positivity was at its lowest across all treatment groups, indicating minimal proliferative activity. The proportion of cells became senescent after treatment followed by washout with Epothilone B (35.4±4.7%), SB-743921 (33.7±3.0%), Paclitaxel (46.9±4.5%), and Vinorelbine (25.2±6.3%). In contrast, Control and Nocodazole treatment followed by washout resulted in almost entirely β–gal–negative cells, consistent with normal proliferative capacity.

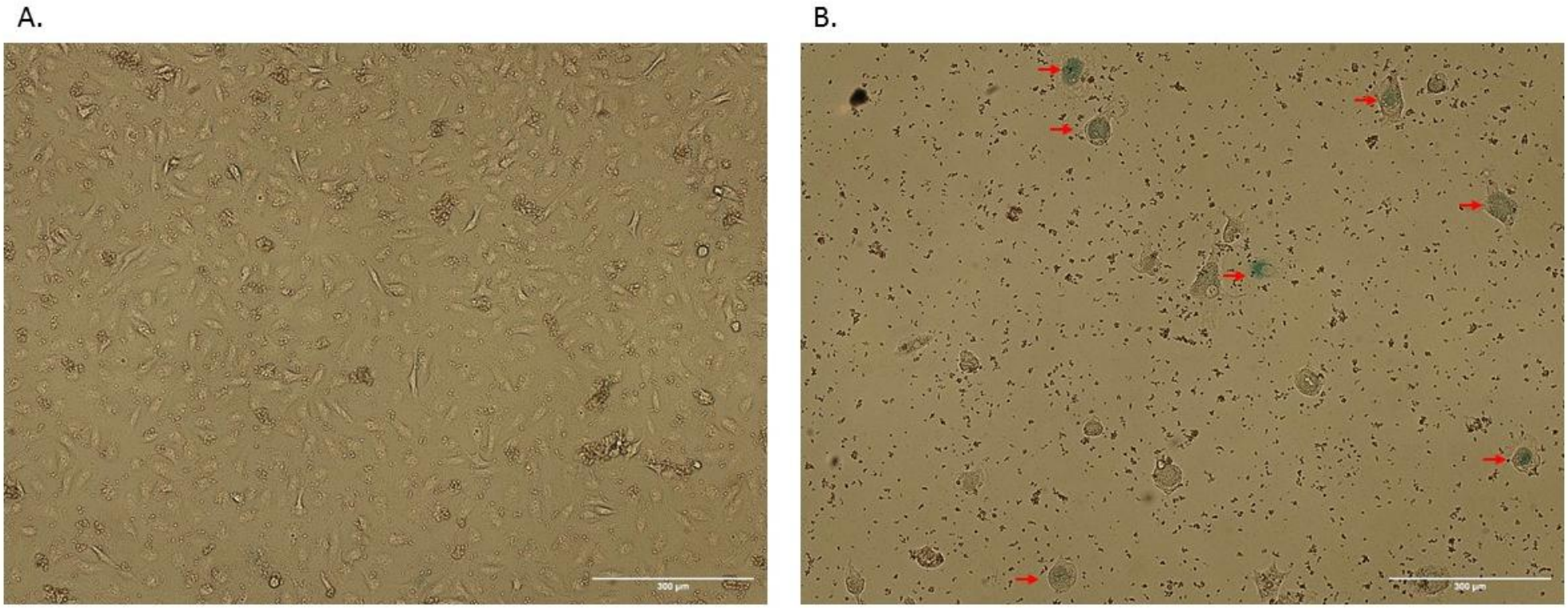

Figure 22. β-galactosidase staining to assess cellular senescence. (A) Control A549 cells show minimal β-gal staining. (B) Cells treated with 300 nM Paclitaxel for 2 hours followed by washout and cultured for 7 days, show increased senescence-associated β-galactosidase activity, indicated by blue-stained cells (red arrows). Scale bars: 300 µm

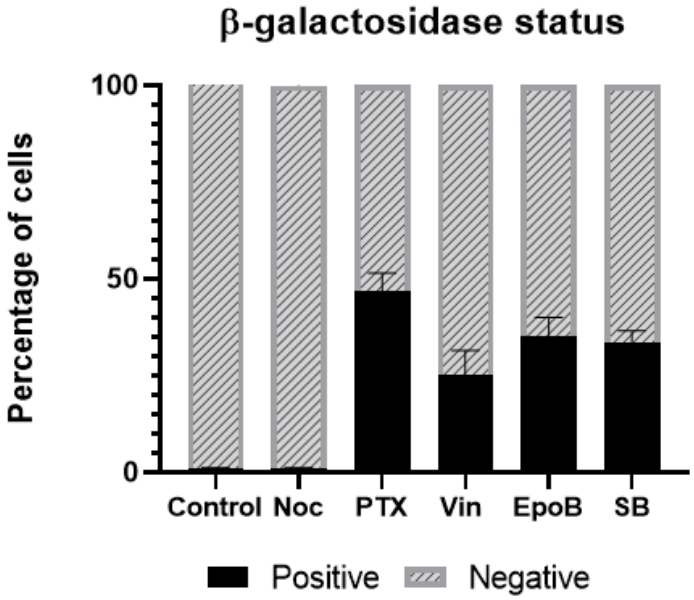

Figure 23. Quantification of β–galactosidase–positive cells 7 days after 2-hour drug treatment followed by washout. The bar graph shows the percentage of senescent (β–gal–positive, black) and non-senescent (β–gal–negative, hatched) A549 cells after treatment followed by washout with the indicated drugs.

Discussion

Overview of Key Findings

Most studies investigating the effects of mitotic inhibitors have relied on prolonged or continuous drug exposure, often extending from 24 to 72 hours (Gascoigne and Taylor, 2008; Suleimenov et al., 2022). However, they do not accurately mimic the real-life scenario of antimitotic agents *in vivo*, where drug exposure is typically short due to rapid metabolism and clearance. Consequently, the long-term effects of short-term treatment remain understudied, particularly in drug-resistant cancer cells, where survival after drug withdrawal may contribute to disease relapse or resistance.

Overall, by using drug concentrations corresponding to the T2 threshold, the lowest dose sufficient to induce mitotic arrest in more than 90% of cells, we demonstrated that even short-term (2-hour) drug exposure can trigger persistent and profound alterations in cell behavior, fate, and long-term proliferative capacity.

Previous work by Suleimenov et al. (2022) demonstrated that defining T1 and T2 threshold doses for microtubule-targeting agents revealed important variability in mitotic responses, which is often overlooked when using excessively high, single drug concentrations. Building on this approach, we confirmed similar dose-dependent behavior for SB-743921 and Epothilone B in A549 cells. Our titration experiments showed that both drugs exhibit clear T2 thresholds that induce robust mitotic arrest with distinct downstream phenotypes, where SB-743921 and Epothilone B treatment resulted in mitotic slippage and mitotic death.

Following drug removal, normal cell behavior was observed only in the Nocodazole treatment group. In all other cases, even cells that entered mitosis after washout failed to undergo normal division. Notably, a short 2-hour exposure was sufficient to induce similar abnormal outcomes, indicating that even brief drug contact can have lasting effects. Analysis of microtubule dynamics revealed that the drugs' primary effects—such as microtubule depolymerization or stabilization—were reversed within 24 hours post-washout. However, abnormal mitosis was present up to at least Day 6, suggesting that the cellular response to these drugs is more complicated than expected. Interestingly, the duration of mitotic arrest following washout was shorter for Nocodazole, Epothilone B, and Paclitaxel treatment groups compared to continuous exposure, further confirming that the drugs were effectively removed. Additionally, this decrease in mitotic duration is not correlated with the outcome of this mitotic arrest/mitosis. Nonetheless, the prolonged persistence of cellular abnormalities indicates that drug-induced effects involve complex mechanisms.

A similar question of reversibility was raised in a recent study of Plk1 inhibitors, where most compounds, such as BI 2536, RO3280, and BI 6727, failed to support full mitotic recovery after washout. Although drug clearance was not directly measured, the authors suggested that incomplete washout may explain the persistent mitotic arrest and failure to divide (Aspinall et al., 2015). Only CYC140844, a selective Plk1 inhibitor, allowed complete recovery, highlighting that drug-specific properties play a critical role in reversibility. Together, these findings suggest that persistent cell cycle defects after short-term treatment can result from transient mitotic disruption, even in the absence of ongoing target inhibition.

Long-term consequences of continuous exposure to mitotic inhibitors have been documented in previous studies (Mittal et al., 2017; Mirzayans et al., 2018), demonstrating the potential for recovery or senescence following drug withdrawal. However, the long-term effects of short-term treatments followed by washout—more reflective of *in vivo* pharmacokinetics—remain poorly understood. Our study shows that even a 2-hour exposure to mitotic inhibitors is sufficient to induce prolonged alterations in cell fate, with distinct recovery patterns depending on the drug. Two forms of recovery were observed, dispersed growth and colony formation, each reflecting differing capacities for clonal repopulation. Nocodazole-treated cells resumed proliferation in a dispersed pattern shortly after washout. In contrast, Paclitaxel, Vinorelbine, and SB-743921 triggered the delayed emergence of cell colonies, which began forming around Days 12 to 15. These colonies likely represent clonal outgrowths from a subset of resistant or escaped cells capable of re-entering the cell cycle after a prolonged arrest. Notably, Epothilone B completely abrogated recovery, as no proliferation or colony formation was observed even 30 days post-washout, suggesting irreversible arrest or commitment to non-proliferative states.

Since mitotic slippage and abnormal divisions typically give rise to multinucleated or abnormally large mononucleated cells, we wanted to assess the dynamics of mononucleated and multinucleated/large mononucleated cells after washout for 18 days. A pronounced decline in mononucleated cells was observed by Day 3 after washout from 2h Paclitaxel, Vinorelbine, and SB-743921 treatments, coinciding with an increase in multinucleated or abnormally large mononucleated cells. This nuclear distortion persisted through Day 6 and gradually reversed by Day 15–18, as mononucleated cells recovered to near-baseline levels. In contrast, Epothilone B induced a persistent multinucleated/large mononucleated state, with no evidence of nuclear normalization, consistent with its failure to support recovery.

Interestingly, a subset of mononucleated cells across treatment groups never entered mitosis within the observation window, especially after short-term exposure. Whether this reflects a true G1 arrest, senescence, or simply a delayed entry remains unclear. The observation of these non-mitotic, large mononucleated cells suggests additional checkpoints may be activated post-washout, possibly involving p21, p16, or ATM/ATR pathways (Kumari et al., 2014; Kulaberoglu et al., 2021). Notably, some of these cells may represent a subpopulation of cancer stem-like cells that are inherently quiescent but capable of surviving cytotoxic stress and re-entering the cell cycle at later time points, thereby contributing to long-term recovery and potential relapse (Mai et al., 2023). Further transcriptomic or proteomic profiling of these non-dividing populations could yield insights into how transient drug exposure rewires cell cycle control.

The recovery of proliferation was further evaluated via Ki67 immunostaining and β-galactosidase senescence assays. As in the distribution of mononucleated and multinucleated/large mononucleated cell dynamics, Paclitaxel, SB-743921, and Vinorelbine induced a marked reduction in Ki67-positive cells by Day 3, followed by partial recovery by Day 18. This delayed re-entry into the cell cycle reflects a transient but drug-specific inhibition of proliferative potential. In contrast, Epothilone B caused a near-complete and persistent suppression of proliferation. This demonstrates that Epothilone B is much more effective compared to other treatment groups in combating cancer. Importantly, β-galactosidase staining revealed a significant proportion of cells entering senescence across all long-acting drugs, particularly Epothilone B and Paclitaxel.

Limitations

While this study provides valuable insights into the long-term consequences of short-term mitotic inhibitor exposure, there are several limitations of this research. First, all experiments were conducted using a single cancer cell line (A549), thus, future studies should replicate the experimental framework in additional cell lines. Also, the *in vitro* nature of this study does not account for the influence of the tumor microenvironment, which plays a critical role in modulating drug response (Rodrigues et al., 2024). As such, extending this work to more physiologically relevant models, such as 3D culture (Edmondson et al., 2014), co-culture systems (Berg et al., 2014), or *in vivo* studies, will be essential to better understand how these findings translate to clinical settings.

Additionally, although this study categorized cells as mononucleated or multinucleated based on morphology, these designations may not fully capture their proliferative potential. Some large mononucleated cells may retain the ability to divide after prolonged arrest, while others are irreversibly senescent. Conversely, not all multinucleated cells are senescent or non-proliferative. Further phenotyping using cell cycle markers, live-cell imaging of division attempts, or lineage tracing would help distinguish reversible arrest from terminal states and clarify the contribution of each subpopulation to recovery or relapse.

Future Perspectives

Nonetheless, this study can have clinical implications after demonstrating the effectiveness of short treatment durations. By understanding how brief drug exposures influence cell fate and recovery after washout, clinicians can optimize and personalize treatment schedules, adjusting clinical doses to the individual patient's needs. This approach has the potential to maximize tumor cell death while minimizing toxicity. The use of short but effective treatments with antimitotic agents can allow additional combinational strategies with, for example, DNA-damaging agents.

For future directions, the next research should focus on the molecular pathways that play a role in this long-term proliferation arrest. Key areas of interest include the roles of tumor suppressor p53 and cell cycle regulators from the Cip/Kip and INK4 families, which may control cell cycle checkpoints.

Conclusion

Our findings demonstrate that even brief exposure to mitotic inhibitors can induce lasting effects on cancer cell fate, including delayed proliferation, accumulation of multinucleated or large mononucleated cells, and senescence. Recovery dynamics were highly drug-specific, with some compounds allowing clonal repopulation and others inducing irreversible arrest. These results underscore the importance of considering both short-term and long-term cellular responses when evaluating anti-mitotic therapies and highlight the need for further investigation into the molecular mechanisms driving recovery versus arrest.

Reference List

Alberts, B., Heald, R., Johnson, A., Morgan, D., Raff, M., Roberts, K., & Walter, P. (2022). Molecular biology of the cell: Seventh International Student Edition with Registration Card. W.W. Norton & Company.

Aspinall, C. F., Zheleva, D., Tighe, A., & Taylor, S. S. (2015). Mitotic entry: Non-genetic heterogeneity exposes the requirement for Plk1. *Oncotarget*, *6*(34), 36472–36488. https://doi.org/10.18632/oncotarget.5507

Berg, E. L., Hsu, Y., & Lee, J. A. (2014). Consideration of the cellular microenvironment: Physiologically relevant co-culture systems in drug discovery. Advanced Drug Delivery Reviews, 69–70, 190–204. https://doi.org/10.1016/j.addr.2014.01.013

Bharadwaj, D., & Mandal, M. (2019). Senescence in polyploid giant cancer cells: A road that leads to chemoresistance. Cytokine & Growth Factor Reviews, 52, 68–75. https://doi.org/10.1016/j.cytogfr.2019.11.002

Bongero, D., Paoluzzi, L., Marchi, E., Zullo, K. M., Neisa, R., Mao, Y., Escandon, R., Wood, K., & O'Connor, O. A. (2015). The novel kinesin spindle protein (KSP) inhibitor SB-743921 exhibits marked activity in in vivo and in vitro models of aggressive large B-cell lymphoma. Leukemia & Lymphoma/Leukemia and Lymphoma, 56(10), 2945–2952. https://doi.org/10.3109/10428194.2015.1020058

Čermák, V., Dostál, V., Jelínek, M., Libusová, L., Kovář, J., Rösel, D., & Brábek, J. (2020). Microtubule-targeting agents and their impact on cancer treatment. *European Journal of Cell Biology*, *99*(4), 151075. https://doi.org/10.1016/j.ejcb.2020.151075

Edmondson, R., Broglie, J. J., Adcock, A. F., & Yang, L. (2014). Three-Dimensional cell culture systems and their applications in drug discovery and Cell-Based biosensors. Assay and Drug Development Technologies, 12(4), 207–218. https://doi.org/10.1089/adt.2014.573

Gampa, G., Kenchappa, R. S., Mohammad, A. S., Parrish, K. E., Kim, M., Crish, J. F., Luu, A., West, R., Hinojosa, A. Q., Sarkaria, J. N., Rosenfeld, S. S., & Elmquist, W. F. (2020). Enhancing Brain Retention of a KIF11 Inhibitor Significantly Improves its Efficacy in a Mouse Model of Glioblastoma. Scientific Reports, 10(1). https://doi.org/10.1038/s41598-020-63494-7

Gascoigne, K. E., & Taylor, S. S. (2008). Cancer Cells Display Profound Intra- and Interline Variation following Prolonged Exposure to Antimitotic Drugs. Cancer Cell, 14(2), 111–122. https://doi.org/10.1016/j.ccr.2008.07.002

Gomez, H. L., Philco, M., Pimentel, P., Kiyan, M., Monsalvo, M. L., Conlan, M. G., Saikali, K. G., Chen, M. M., Seroogy, J. J., Wolff, A. A., & Escandon, R. D. (2011). Phase I dose-escalation and pharmacokinetic study of ispinesib, a kinesin spindle protein inhibitor, administered on days 1 and 15 of a 28-day schedule in patients with no prior treatment for advanced breast cancer. Anti-Cancer Drugs, 23(3), 335–341. https://doi.org/10.1097/cad.0b013e32834e74d6

Fanale, D., Bronte, G., Passiglia, F., Calò, V., Castiglia, M., Di Piazza, F., Barraco, N., Cangemi, A., Catarella, M. T., Insalaco, L., Listì, A., Maragliano, R., Massihnia, D., Perez, A., Toia, F., Cicero, G., & Bazan, V. (2015). Stabilizing versus Destabilizing the Microtubules: A Double-Edge Sword for an Effective Cancer Treatment Option? *Analytical Cellular Pathology*, *2015*, 1–19. https://doi.org/10.1155/2015/690916

Gregory, R. K., & Smith, I. E. (2000). True. *British Journal of Cancer*, *82*(12), 1907–1913. https://doi.org/10.1054/bjoc.2000.1203

Komlodi-Pasztor, E., Sackett, D. L., & Fojo, A. T. (2012). Inhibitors Targeting Mitosis: Tales of How Great Drugs against a Promising Target Were Brought Down by a Flawed Rationale. Clinical Cancer Research, 18(1), 51–63. https://doi.org/10.1158/1078-0432.ccr-11-0999

Kowalski, R. J., Giannakakou, P., & Hamel, E. (1997). Activities of the Microtubule-stabilizing Agents Epothilones A and B with Purified Tubulin and in Cells Resistant to Paclitaxel (Taxol®). *Journal of Biological Chemistry*, *272*(4), 2534–2541. https://doi.org/10.1074/jbc.272.4.2534

Kulaberoglu, Y., Hergovich, A., & Gómez, V. (2021). The role of p53/p21/p16 in DNA damage signaling and DNA repair. In Elsevier eBooks (pp. 257–274). https://doi.org/10.1016/b978-0-323-85679-9.00015-5

Kumari, G., Ulrich, T., Krause, M., Finkernagel, F., & Gaubatz, S. (2014). Induction of p21CIP1 Protein and Cell Cycle Arrest after Inhibition of Aurora B Kinase Is Attributed to Aneuploidy and Reactive Oxygen Species. *Journal of Biological Chemistry*, *289*(23), 16072–16084. https://doi.org/10.1074/jbc.m114.555060

Lad, L., Luo, L., Carson, J. D., Wood, K. W., Hartman, J. J., Copeland, R. A., & Sakowicz, R. (2008). Mechanism of inhibition of human KSP by Ispinesib. Biochemistry, 47(11), 3576–3585. https://doi.org/10.1021/bi702061g

Mai, Y., Su, J., Yang, C., Xia, C., & Fu, L. (2023). The strategies to cure cancer patients by eradicating cancer stem-like cells. *Molecular Cancer*, *22*(1). https://doi.org/10.1186/s12943-023-01867-y

Mirzayans, R., Andrais, B., & Murray, D. (2018). Roles of Polyploid/Multinucleated giant cancer cells in metastasis and disease relapse following anticancer treatment. Cancers, 10(4), 118. https://doi.org/10.3390/cancers10040118

Mittal, K., Donthamsetty, S., Kaur, R., Yang, C., Gupta, M. V., Reid, M. D., Choi, D. H., Rida, P. C. G., & Aneja, R. (2017). Multinucleated polyploidy drives resistance to Docetaxel chemotherapy in prostate cancer. British Journal of Cancer, 116(9), 1186–1194. https://doi.org/10.1038/bjc.2017.78

Mustyatsa, V. V., Kostarev, A. V., Tvorogova, A. V., Ataullakhanov, F. I., Gudimchuk, N. B., & Vorobjev, I. A. (2019). Fine structure and dynamics of EB3 binding zones on microtubules in fibroblast cells. Molecular Biology of the Cell, 30(17), 2105–2114. https://doi.org/10.1091/mbc.e18-11-0723

Novais-Cruz, M., Pombinho, A., Sousa, M., Maia, A. F., Maiato, H., & Ferrás, C. (2023). Mitotic DNA damage promotes chromokinesin-mediated missegregation of polar chromosomes in cancer cells. Molecular Biology of the Cell, 34(5). https://doi.org/10.1091/mbc.e22-11-0518

Rodrigues, D. B., Reis, R. L., & Pirraco, R. P. (2024). Modelling the complex nature of the tumor microenvironment: 3D tumor spheroids as an evolving tool. Journal of Biomedical Science, 31(1). https://doi.org/10.1186/s12929-024-00997-9

Sati, P., Sharma, E., Dhyani, P., Attri, D. C., Rana, R., Kiyekbayeva, L., Büsselberg, D., Samuel, S. M., & Sharifi-Rad, J. (2024). Paclitaxel and its semi-synthetic derivatives: comprehensive

insights into chemical structure, mechanisms of action, and anticancer properties. *European Journal of Medical Research*, *29*(1). https://doi.org/10.1186/s40001-024-01657-2

Suleimenov, M., Bekbayev, S., Ten, M., Suleimenova, N., Tlegenova, M., Nurmagambetova, A., Kauanova, S., & Vorobjev, I. (2022). Bcl-xL activity influences outcome of the mitotic arrest. Frontiers in Pharmacology, 13. https://doi.org/10.3389/fphar.2022.933112

Was, H., Borkowska, A., Olszewska, A., Klemba, A., Marciniak, M., Synowiec, A., & Kieda, C. (2022). Polyploidy formation in cancer cells: How a Trojan horse is born. *Seminars in Cancer Biology*, *81*, 24–36. https://doi.org/10.1016/j.semcancer.2021.03.003

Weaver, B. A. (2014). How Taxol/paclitaxel kills cancer cells. Molecular Biology of the Cell, 25(18), 2677–2681. https://doi.org/10.1091/mbc.e14-04-0916

List of Tables

List of Figures

Conference presentations

Poster presentation:

Orazbek, A., Janibekova, M., Yelzhanov, A., Kutchanova, M., Yeskendirova, R., Anapina, A., & Vorobjev, I. (2024). Prolonged Inhibition of Cell Proliferation by Short-Term Exposure With Certain Anti-Microtubule Drugs. In *ICKSMCB 2024* [Poster presentation]. https://www.ksmcb.or.kr/icksmcb2024/about/sub01.html

Appendices

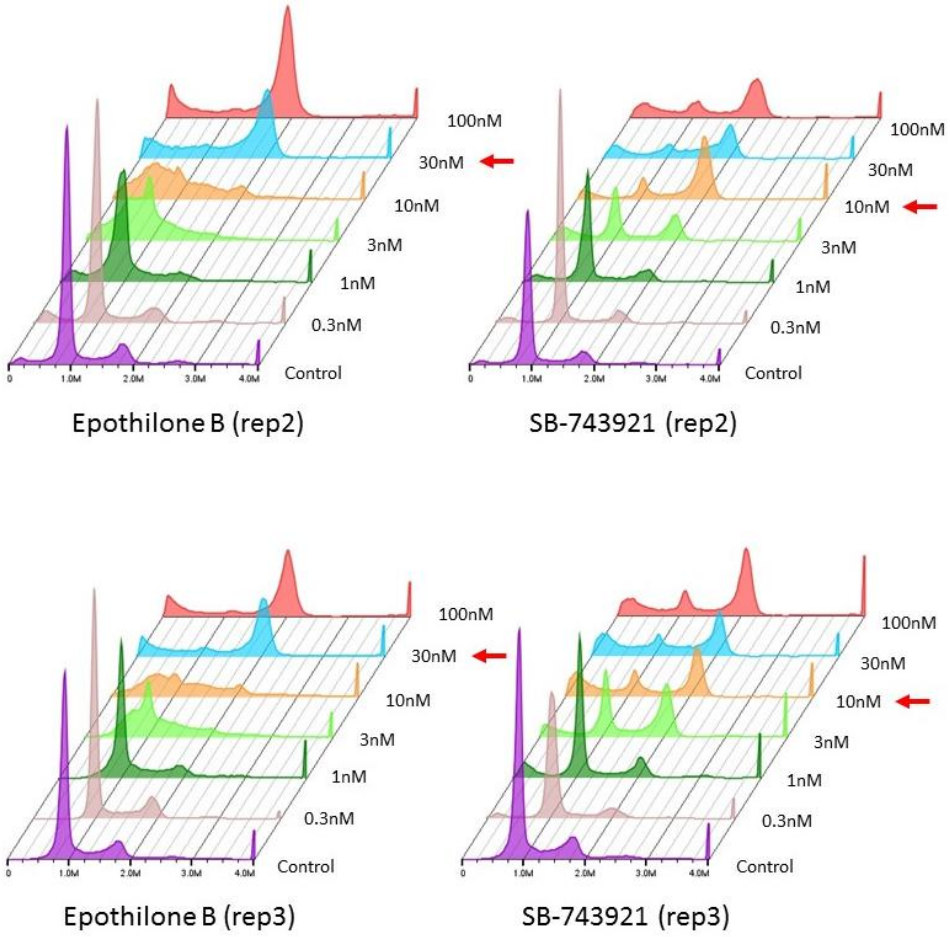

Supplementary Figure 1. Titration of Epothilone B and SB-743921 in A549 cells: two other biological repeats. DNA content histograms after 24-hour treatment with increasing concentrations of Epothilone B (left) and SB-743921 (right). Arrows indicate selected T2 concentrations (30 nM for Epothilone B, 10 nM for SB-743921) that induce mitotic arrest (significant accumulation in G2/M) (N> 30,000).

Supplementary Table 1. Statistical Analysis (2-way ANOVA with Dunnett's test) Data for Cell Number Change Comparison After 2h Treatment with Mitotic Inhibitors Followed by Washout

Dunnett's multiple comparisons test		Significant?	Summary	Adjusted P Value
Control	Day 1 vs. Day 3	No	ns	0.2416
	Day 1 vs. Day 6	Yes	****	<0.0001
Noc	Day 1 vs. Day 3	No	ns	0.9703
	Day 1 vs. Day 6	Yes	****	<0.0001

Dunnett's multiple comparisons test		Significant?	Summary	Adjusted P Value
Vin	Day 1 vs. Day 3	No	ns	>0.9999
	Day 1 vs. Day 6	No	ns	0.8833
PTX	Day 1 vs. Day 3	No	ns	0.9382
	Day 1 vs. Day 6	No	ns	0.9521
EpoB	Day 1 vs. Day 3	No	ns	>0.9999
	Day 1 vs. Day 6	No	ns	0.8735
SB	Day 1 vs. Day 3	No	ns	0.9622
	Day 1 vs. Day 6	No	ns	0.9972

Supplementary Table 2. Statistical Analysis (One-way Welch's ANOVA with Dunnett's T3 test) Data for EB3 comet Speed Difference After 2h Treatment with Mitotic Inhibitors Followed by Washout

Dunnett's T3 multiple comparisons test	Significant?	Summary	Adjusted P Value
Control vs. 2h	Yes	**	0.0038
Control vs. 1 day	No	ns	0.9995
Control vs. 2h	Yes	****	<0.0001
Control vs. 1 day	No	ns	0.1209
Control vs. 2h	Yes	****	<0.0001
Control vs. 1 day	No	ns	0.9452
Control vs. 2h	Yes	****	<0.0001
Control vs. 1 day	Yes	*	0.0309
Control vs. 2h	Yes	****	<0.0001

Control vs. 1 day	No	ns	0.9931
Control vs. 2h	Yes	****	<0.0001
Control vs. 1 day	No	ns	0.2661

Supplementary Table 3. Statistical Analysis (Kruskal-Wallis test with Dunnett's test) for Mitotic Arrest Duration Comparison

Dunn's multiple comparisons test	Significant?	Summary	Adjusted P Value
Control vs. Noc 1uM in drug	Yes	****	<0.0001
Control vs. Noc 1uM 16h	No	ns	>0.9999
Control vs. Noc 1uM 2h	No	ns	>0.9999
Control vs. PTX 300nM in drug	Yes	****	<0.0001
Control vs. PTX 300nM 16h	Yes	**	0.0028
Control vs. PTX 300nM 2h	Yes	**	0.0016
Control vs. EpoB 30nM in drug	Yes	****	<0.0001
Control vs. EpoB 30nM 16h	Yes	***	0.0001
Control vs. EpoB 30nM 2h	No	ns	>0.9999
Control vs. Vin 1uM in drug	Yes	****	<0.0001
Control vs. Vin 1uM 16h	Yes	****	<0.0001
Control vs. Vin 1uM 2h	Yes	****	<0.0001
Control vs. SB 10nM in drug	Yes	****	<0.0001
Control vs. SB 10nM 16h	Yes	****	<0.0001
Control vs. SB 10nM 2h	Yes	****	<0.0001
Noc 1uM in drug vs. Noc 1uM 16h	Yes	****	<0.0001

Dunn's multiple comparisons test	Significant?	Summary	Adjusted P Value
Noc 1uM in drug vs. Noc 1uM 2h	Yes	****	<0.0001
PTX 300nM in drug vs. PTX 300nM 16h	Yes	****	<0.0001
PTX 300nM in drug vs. PTX 300nM 2h	Yes	****	<0.0001
EpoB 30nM in drug vs. EpoB 30nM 16h	Yes	****	<0.0001
EpoB 30nM in drug vs. EpoB 30nM 2h	Yes	****	<0.0001
Vin 1uM in drug vs. Vin 1uM 16h	No	ns	>0.9999
Vin 1uM in drug vs. Vin 1uM 2h	Yes	***	0.0001
SB 10nM in drug vs. SB 10nM 16h	No	ns	>0.9999
SB 10nM in drug vs. SB 10nM 2h	No	ns	0.7188